Sudan University of Science & Technology

Collage of petroleum Engineering

Exploration petroleum Engineering Department.

# *Petrophysical determination and lithological Identification using multi well logging methods in kiakange wells (1, 2 and 3) in Tendi formation Muglad basin _Sudan.*

Graduation project submitted to the collage of petroleum Engineering & Technology, Sudan of University Science & Technology.

Partial requirement for a B.sc Degree in Exploration petroleum Engineering.

Prepared by:

1. El muiz Jamal Mahmoud Mohamed.

2. Mohammed Al ballal Abd almajed Al amein.

3. Mojahid Elsheikh Mohamed Ahmed Al hassan.

4. Tarig Mahjoub Mahmoud Mohammed.

5. Wadah Ahmed Abd Elmajed Hmid

This project has been approved by the collage of petroleum engineering & technology.

Signature……..

Project supervisor.

Tch. Mohamed Salah Ahmed El Emam

Signature…….

Director of Exploration petroleum Engineering Department.

Tch. Mohamed abdallah

Signature……

Dean of collage of petroleum Engineering & Technology.

Dr. Tagwa Ahmed.

Signature……...

Date……

# الاستهلال

قال الله تعالي:

{وَلَوْ أَنَّمَا فِي الْأَرْضِ مِن شَجَرَةٍ
أَقْلَامٌ وَالْبَحْرُ يَمُدُّهُ مِن بَعْدِهِ
سَبْعَةُ أَبْحُرٍ مَّا نَفِدَتْ كَلِمَاتُ
اللَّهِ ۗ إِنَّ اللَّهَ عَزِيزٌ حَكِيمٌ}

صورة لقمان الأيه "27"

وقال الامام الشافعي:

(أخي لن تنال العلم إلا بست سأنبئك عن
تفصيلها ببيان ،ذكاء وحرص واجتهاد
وبلغة وصحبة أستاذ وطول زمان)

# الإهداء

من مكنونات أعماق القلب

إلى.....الذي ضحى بكل عمره وظل رمزا للتفاني والعطاء

أبي

إلى.....التي الجنة من تحت أقدامها التي ظلت نبعاً أماناً حناناً دفاقاً لكل جميل

كانت أبداً مثلا للمثابة

أمي

إلى.....الذين يتمنون لنا صادق وأعذب الأمنيات الجميلات الرائعات

أخواني وأخواتي

إلى.....رفقاء الدرب وأعزاء القلب من كانوا نوراً لمسيرة نجاحي وكل باحث

عن العلم والمعرفة

أصدقائي

إلى.....الذين سطروا فوق جبيننا أسمى معاني البذل والإخلاص

أساتذتي الأجلاء

**الى..... من كان رمزا للوفاء وللاخلاص الى روح الفقيد**

**الدكتور محمد نعيم عليه رحمة الله**

قم للمعلم وفه التبجيل كاد المعلم أن يكون رسولا

نهدي ثمرة جهدنا نتمنى أن ينال رضاكم

# الشـــكر والعرفـان

الشكر أولا وأخيرا لله رب العالمين

ثم الشكر لصرح العلم والمعرفة جامعة السودان للعلوم والتكنولوجيا

تقديرنا العظيم لي أساتذتنا الأجلاء الذين لولا جهدهم وعونهم لنا بعد عون الله لما كان هذا الجهد أن يري النور

إن ألسنتنا لتعجز عن الثناء عليهم ونقول لهم أن شكلنا إضافة في حقل تخصصنا فلهم أن يفخروا بنا

حتما سنكون كما أرادوا لنا ...رجال علي قدر أهل العزم

ونخص باسمي آيات الشكر والامتنان للأستاذ/محمد صلاح احمد الإمام الذي وجدناه أخا وصديقا عزيزا كرس لنا جم جهده و وقته وكان خير معيناً لنا بعد الكريم عز وجل.

كما نخص بالشكر أيضا الأستاذ /عمرو يوسف الذي كان خير قدوة لنا خلال مسيرتنا العلمية

وكذلك نشكر الأستاذ الفاضل/عثمان مالك الذي ساعدنا في إخراج هذا البحث.

# ABSTRACT

The study area located in the north west of Unity State, south central of Muglad Rift Basin. It is bounded approximately by Latitudes $09^{o}17'$ and $09^{o}26'$ N and Longitudes $29^{o}$ 5' and $29^{o}10'$ E

A simplified interpretation has been established from integrated well data, lithology logs, porosity logs and resistivity logs data focusing on Tendi formation in the Kaikange area in the Muglad Basin, southern Sudan.

Tendi formation characterized by intercalated between thin sandstone and claystone beds with good porosity in sandstone, the porosity average is more than 28 %. In this study many zones were selected showing good indicator of porosity and saturation.

# التجريد

تقع منطقة الدراسه في الجزء الجنوبي الغربي من ولاية الوحده ، الجنوبي المركزي من حوض المجلد . بخطوط طول'17 $09^{o}$ و '26 $09^{o}$ ش ، ودوائر عرض '05 $29^{o}$ و '10 $29^{o}$ ق.

أجريت بعض التفسيرات من معلومات الابار والتسجيلات الصخريه (lithology logs) وكذلك تسجيلات المقاومية (Resistivity logs)والمسامية(Porosity logs) على تكوين تندي في ابار كيكانج من حوض المجلد في الجزء الجنوبي من السودان .

يتميز تكوين تندي بوجود طبقات رقيقه متداخلة من الحجر الطيني والحجر الرملي ذو المسامية الجيده .في النطاقات المختاره في منطقة الدراسة متوسط المساميه يصل الي اكثر من 28% كما توجد عدت نطاقات ذات مؤشر جيد للتشبع والمساميه .

# Table of Contents

# LIST OF FIGURES

# LIST OF TABLES

# CHAPTER ONE
# INTRODUCTION

# 1 Introduction

## 1.1 Location of study area:

The Muglad Rift Basin is the largest of the Central African Rift basins located in southwest central Sudan. It covers an area about 120,000 $km^2$ and is up to 200 km wide and over 800 km long. Locally the basin contains up to 13 km of Cretaceous to Tertiary sediments. It extends from western Kordofan, to southern Darfur States in the. It contains a number of hydrocarbon accumulations of various sizes, the largest of which are the Heglig and Unity oil field, the Kaikang Trough (present study area) is located in the north west of Unity State, south central of Muglad Rift Basin. It is bounded approximately by Latitudes $09^o17'$ and $09^o26'$ N and Longitudes $29^o$ 5' and $29^o10'$ E (Fig.1.1). Muglad Basin is a rift basin developed in Mesozoic-Cenozoic time and was initiated as an extensional basin or graben (half-graben) to the direct south of the Central African Shear Zone (CASZ).The Muglad town it's in a western Kordofan state, Muglad town represent the center town of the Messeria tribe.

Three wells from the study area were selected for the present study, namely Kaikang-1, Kaikang-2 and kaiknge-3.

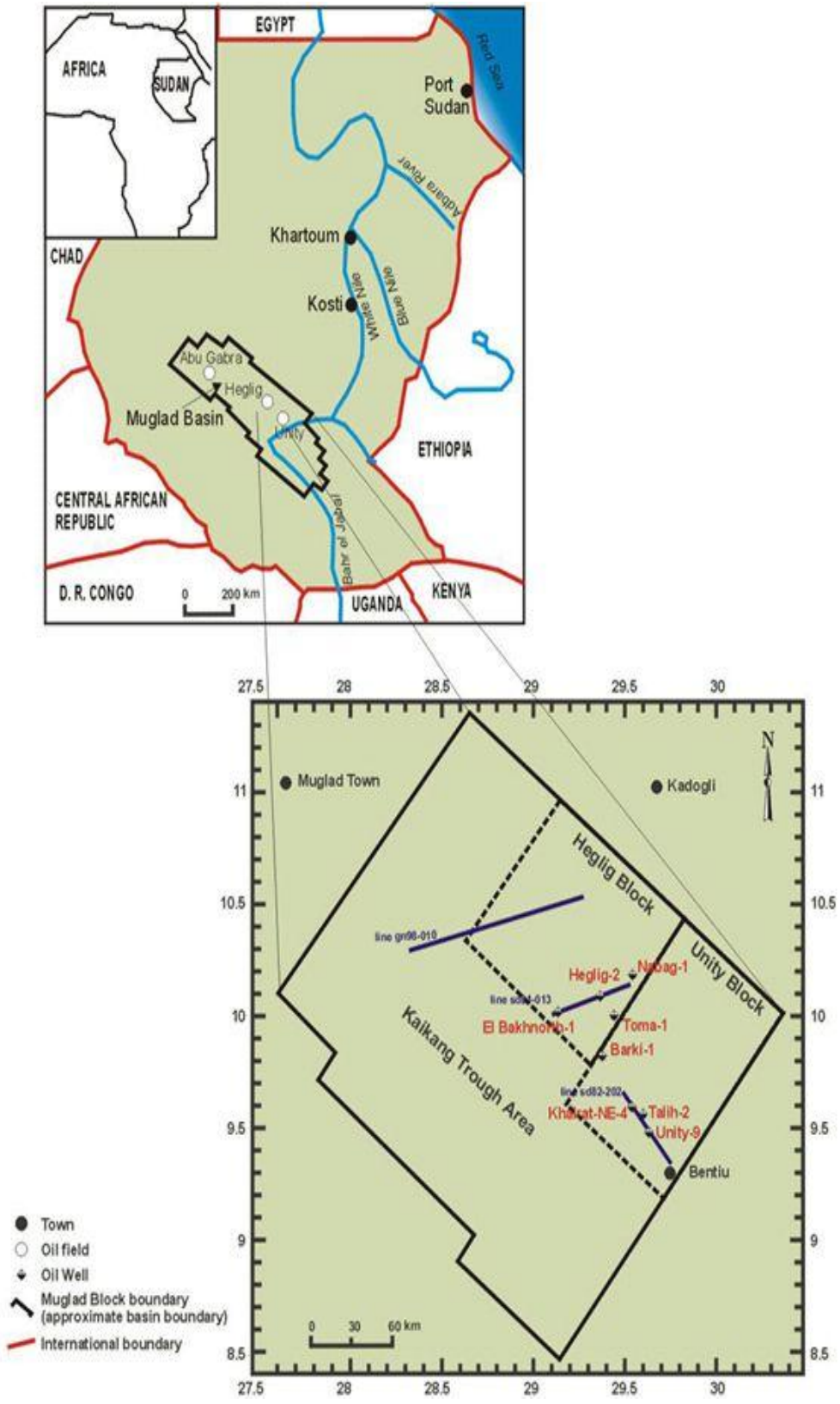


Figure1. : Shows the location of study area1

## 1.2 Accessibility:

The study area is linked with Khartoum by a railway line which passes through Sennar, Kosti, ErRahad to Babanusa and then runs southward through the Muglad city to Wau. Also from Babanusa a line runs westward via the NW Muglad Basin up to Nyala. A paved road runs from Khartoum to Kadugli through El Obeid, but from El Obeid many unpaved roads can be followed to different towns and villages in the area. These passageways cross thick forest and mountainous areas and are passable only during the dry season. Also we could reach it by airplanes which are safest, fastest and more reliable compared to ground roads.

## 1.3 Topography:

The topography of the study area is characterized by sand dunes which occupy more than 65% of the northern parts of Darfur and about 10 to 15% of southern Darfur. The region is characterized by gently undulating to nearly level uplands; however, it is interspersed with various hills and mountains. The mountainous and hilly trains occupy some areas of central Darfur and featured mainly by the massive Jebel Marra and other hills such as Meidoub and Tagabo. Clay and Gardud soils occupy the western and south western parts and some areas in the north.

## 1.4 Drainage:

The White Nile and its tributaries which are Bahr El Arab, Bahr El Gazal and Bahr El Zaraf are the major drainage in the area .The White Nile is flowing across the southern and the eastern parts of the Muglad Basin. The southern part of the White Nile River is called Bahr El Jabal. The Kordofan and Darfur surface water drainage systems are mostly seasonal streams. Khor Abu Habel and WadiKhadari represent the most significant drainage system in the area. Some of the small spring-fed streams and of the ephemeral wadis and khors which carry runoff reach the White Nile or its perennial tributaries.

## 1.5 Climate:

The southern Central Sudan is generally considered to have Savannah-type climate where the average annual precipitation ranges between 120 and 800 mm. This Savannah-type climate shows a gradual change from the very humid southern equatorial climate to the semi-arid northern zone. The majority of the rainfall happens normally during July, August and September. The annual rainfall is irregular especially during the last decades when more dry seasons than expected occurred,

causing a regional drought and desertification. The prevailing winter wind comes from the North while that during the rainy season comes from the Southwest. Wind velocities are usually less than 8 km/h. The average daytime temperature reaches approximately 38°C in May and September. In winter (December–March) the temperatures are lower, around 20° – 25°C. The mean humidity ranges from about 21% in the dry season to an average of 75% during the rainy season, Smith (1949) and Harrison and Jackson (1958).

## 1.6 Objective of study:

This study deals with the calculation of petro-physical properties from wire line logs (i.e. Gamma ray log, resistivity logs, and porosity logs) and the data used in this research taken from (Tendi) formation in Muglad basin to define the following

- Identification the lithology of Tendi formations.
- Calculation the formation properties (i.e. porosity, water saturations) and shale volume.

## 1.7 Problem statement:

Tendi formation located in the upper part of sequence in Muglad basin in middle of Miocene. Also the thin sandstone-mudstone intercalated bedding are good reasons most of the previous studies conducted on the source rock in this formation. So in this research we tried to focusing on the formation properties and suggest zones contain water, oil and gas.

## 1.8 Previous study:

The northwest termination of the southern Sudan rifts is at the Central African Shear Zone (CASZ) (Browne and Fairhead, 1983; Browne et al., 1985; Fairhead, 1986). To the southeast, they tend to funnel together, and their extension further south- east is obscured by later Cenozoic volcanic rocks (Bosworth, 1992). Some volcanism is present in the Muglad Basin but is a minor component of the geology in comparison with the Tertiary rifts of East Africa (Fairhead, 1986). Thin basalts were encoun- tered in the centre of the Muglad Basin and dated 82 +2 Ma (Schull, 1988) and aeromagnetic data suggests that volcanics underlie the southwest flank of the structural high linking the Heglig and Unity Fields (McHargue et al., 1992). To the south of the CASZ, lithospheric extension in a northeast to southwest direction over

all the basins amounts to a total of - 100 km in contrast to the area north of the CASZ, where it is much less (Ibrahim et al., 1996).

Browne and Fairhead (1983) first reported on the main features of the Muglad Basin, estimating its depth from gravity data alone as -4.5 km and the maximum amount of crustal extension as 48 km. They pointed out that the thinning of the crust beneath the rifts causes a regional gravity high within which sits the negatwe anomaly of the rift basin.

Schull (1988), Mann (1989) and McHargue et al. (1992) discussed the stratigraphy and structure of central African basins in the light of petroleum exploration in the area. The Muglad Basin is the most extensively explored and proved to contain as much as 13 km of sediment. An extension of 32% for the southern Muglad Basin was estimated from the amount of basin infill, and a depth of 12-16 km was estimated for detachment within the crust.

Schull, (1988) summarized the geochemical data of Chevron Overseas Inc. including routine analyses of whole -rock pyrolysis and organic carbon content based on thousands of rock samples from 65 wells. The analytical data indicate that dark grey lacustrine claystones and shales of the early rift phase (Neocomian-Albian) are moderately rich oil prone source rocks. Total organic carbon content average 1.3% (range 1to 5%). The primary source of kerogn are degraded algal and plant material. During thermal maturation, this hydrogen –rich kerognes generate paraffinic, low sulfur, high pour- point oils. The oils have 18°-45°API gravities and 80°-105° F (45°-59° C) pour points. (Schull, op. cit.)Drew a geochemical log in which the various columns indicate the oil – prone nature of the source rocks HI (Hydrogen Index), the source potential (S2) and the maturation level (Ro).

Robertson Research International (RRI, 1990) evaluated the previous work of Chevron Overseas Inc in the interior rift basins in Sudan and presented a volume en titled The Geology and Petroleum Potential of South, Central and Eastern Sudan. In their study they used various geochemical techniques to evaluate source rock potentiality for hydrocarbon generation.

# CHAPTER TWO

# TECTONIC SETTING AND GEOLOGY

## 2 Tectonic Setting and Geology

From geophysical investigations, palynological and well log data, it has been determined that the interior basins in the southern half of Sudan are broadly Mesozoic to Tertiary in age and have developed as a result of fault controlled subsidence (RRI,1990). The largest basinbeing represented by NW- SE trending Muglad Rift Basin complex and the NNW-SSE trending Melut basin complex. A number of subsidiary basins are associated with these major basins trends; the Rakuba and Jonglie basins representing the extensions of the Muglad Rift Basin complex, whilst the Ruat and Pibor basin represent extension of the Melut basin complex. The Bagara, Nahud, Um Hani and Mahbuba basin are developed above a major WSW-ENE trending lineament across which the Melut and Muglad basin complexes do not continue northwest (RRI,1999). The extensional tectonism that formed these basins began in the Jurassic (?) –Early Cretaceous (Schull, 1988). Movement along major fault trends continued intermittently into the Miocene (Schull). This deformation resulted in a complex structural history that led to the formation of several deep faults–bounded troughs, major inter-basinal highs, and complex basin flanks. This tectonism has created a wide variety of structures many of which become effective hydrocarbon traps. The sedimentary basins of interior Sudan are characterized by thick nonmarineclastic sequences of Jurassic (?)–Early Cretaceous and Tertiary age. Over 45,000 ft (1,716m) of sediment were deposited in the deepest trough and extensive basinal areas are underlain by more than 20,000 ft (6,096m) of sedimentary rocks. The depositional sequences include thick lacustrine shales and claystones, floodplain claystones and lacustrine, fluvial, alluvial sandstone and conglomerate. The lacustrine claystones deposited in a suboxic environment provide good oil –prone source rocks. Reservoir sandstones have been found in a wide variety of non-marine sandstone facies (Schull, 1988). The initiation of rifting in southern Sudan may have been directly related to Jurassic rifting in the Lamu embayment of Kenya (Reeves et al, 1987, Schull). Anza trough of northern Kenya strikes in the same direction as the Muglad, Melut and Blue Nile basins, This primary southern Sudan rifting phase continued into the Albian, corresponding with the initial opening of the south Atlantic and extension in the Benue trough (Wright, 1981). During this period of regionally widespread rifting, thick sedimentary sequences were deposited in several developing

African basins, e.g., Benue trough, East Niger basin, Doba basin, Ngaoundere Rift basin, and Anza trough. Some of these basins developed within and immediately adjacent to the Cretaceous shear zones and others formed near their endpoints at angles of 90°-120º to the shear movement. Fairhead and Green suggested that the movement along the Central African Shear Zone translated into the extensional basins of southern Sudan. This relationship is similar to that between the axial shear zone of the Benue trough and the East Niger rift basin. This mechanism could explain rift basin development contemporaneous with movement along the West and Central African shear zones. The second southern Sudan rifting phase began in the Turonian and continued until near the end of the Cretaceous. This rifting was accompanied by the deposition of up to 6,000 ft (1, 829 m) of sediment, Fairhead has concluded that changes in the opening of south Atlantic account for a late Cretaceous period of shear movement on the West and Central African rift system. This movement could explain Late Cretaceous Benue compression and dextral reactivation of the Central African Shear Zone. The second Sudan rifting phase may be related to this movement (Schull, 1988).In the ENE-WSW trending Bagarra basin, a continuation of the Central African Shear Zone strike-slip movement occurred. This continuing strikeslip movement is not seen in the adjoining north western Muglad basin or further northeast. The ENE-WSW trend appears to have been terminated and replaced by the northwest-southeast trending basins interpreted to be extensional in their development, supporting the concept of translation of shear movement extension. Also during this period rifting and deposition continued in the northwest southeast-trending Anza trough. The thick highly faulted lower Tertiary section of the southern Sudan basins indicates that the final rifting phase was a significant tectonic event. Regional data suggest the initiation of this phase was generally time equivalent to initial phases of the opening of the Red Sea (Lowell and Genik, 1972) and East African Rifting (Girdler, 1969). The Muglad, Melut and Blue Nile basins are subparallel to the Red Sea which rifted in response to the African Arabian extensional forces. A direct relation between the east African rifting and the development of the southern Sudan basins is not apparent interestingly, a sharp contrast is seen between the Tertiary development of southern Sudan basins and the West African basins, which exhibited strong Cretaceous similarities. For example, the East Niger basin (Fig. 3) has only a thin relatively unfaulted Tertiary section (Avbovbo et al, 1986). This section indicates that the significant early Tertiary extension affecting southern Sudan and resulted in the accumulation of over 13,000 ft

(3,962m) of sediment, was inoperative in West Africa basins. However, the Anza trough, to the southeast, did experience rifting and thick accumulation

During late Tertiary, the regional stress regime changed resulting in the Middle Miocene termination of southern Sudan rifting. To the northeast, the Red Sea rift continued its development.

Structural Setting: According to Schull (1988) the structure development of this area can be divided into a pre-rifting phase, three rifting phase and a sag phase

Pre-rifting Phase: By the end of the Pan-African orogeny (550+100 m.y.) this region had become a consolidated platform during the Paleozoic and early Mesozoic. This highland platform provided poorly sorted and various types of sediments to the adjacent subsiding areas, which is called the pre-rifting sediments.

Rifting Phases: Three distinct periods of rifting occurred in response to crustal extension, which provided the isostatic mechanism for subsidence (Browne and Fairhead, 1983, Schull, 1988). Subsidence was accomplished by normal faulting parallel and sub-parallel to the basinal axes and margins. Based on widely spaced penetration, rifting is thought to have begun in the Jurassic (?)-Early Cretaceous (130-160 Ma). This initial and strongest rifting phase lasted until near the end of the Albian. The second rifting phase occurred during the Turonian to late Senonian. This phase resulted in the deposition of lacustrine and floodplain claystones and siltstones which terminated the deposition of Bentiu Formation. The rifting phase was accompanied by minor volcanism .The end of this phase is marked by deposition of an increasing sand-rich sequence that ended with a thick Paleocene sandstone of the Amal Formation. The final rifting phase began in the late Eocene-Oligocene. This final phase is reflected by a thick sequence of lacustrine and floodplain clayey sand stones and siltstones. After this period of rifting deposition became more sand rich throughout the late Oligocene-Miocene (Schull, 1988).

Sag Phase: In the Middle Miocene the basinal areas entered an intracratonic sag phase of very gentle subsidence accompanied by little or no faulting. During this time extensive volcanism occurred in some adjoining areas to the north e.g., Jebel Marra, Meidoub Hills and in the East African Rift system to the east and southeast (Schull, op.cit).

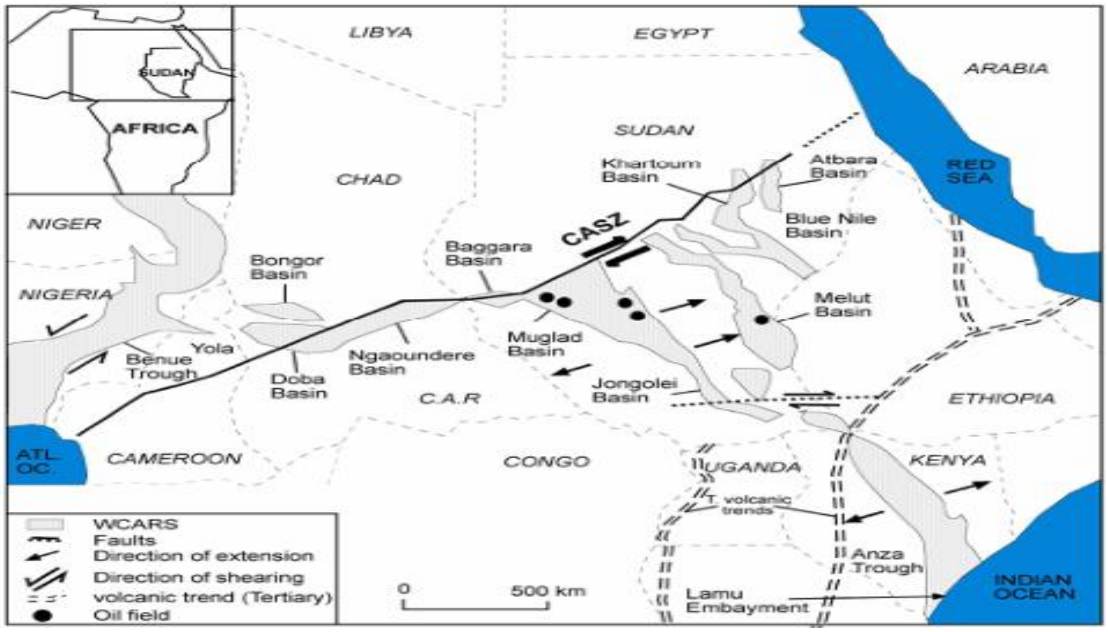


2.1 Figure: Tectonic and Structure Map of the Central African Shear Zone (CASZ), After Fairhead, (1988).

## 2.1 The Stratigraphy Of Mugled Rift Basin:

The major stratigraphic units of the Muglad Rift Basin include the following units. Table is a generalized lithostratigraphic scheme of the basin

## 2.2 Basement Complex (precamberian):

The basement is predominantly made up of Precambrian Cambrian metamorphic rocks with limited occurrences of foliated intrusive igneous rocks including granitic and granodioritic gneiss which has been penetrated only in two wells Baraka 1 and Adilla -1. In Adilla the basement consists of granite overlain by highly lithified sandstone on top while in Baraka the granodiorite gave an age of 540 Ma ± 40 m.y. (Moniem et al., 1984, Schull, 1988).

## 2.3 Cretaceous Sedimentary Units:

A few Nubian sandstone outcrops are encountered in the Muglad basin east and northeast of Muglad town. In this area, the rocks are water laid, non-marine, massively bedded, highly weathered, and medium to coarse grain sandstone. The depositional history and age was difficult to determine, because they from limited and scattered outcrops (Schull, 1988). In the subsurface, a thick sequence of Cretaceous sediment has been penetrated. Based on seismic data and well control, an estimated 20,000 ft (6,096 m) of Cretaceous sediment has been deposited in the deepest troughs (Schull)

Table (2.1) Generalized lithostratigraphical scheme of Muglad Rift Basin (modified by CPL 2009, after Awad, 1999).

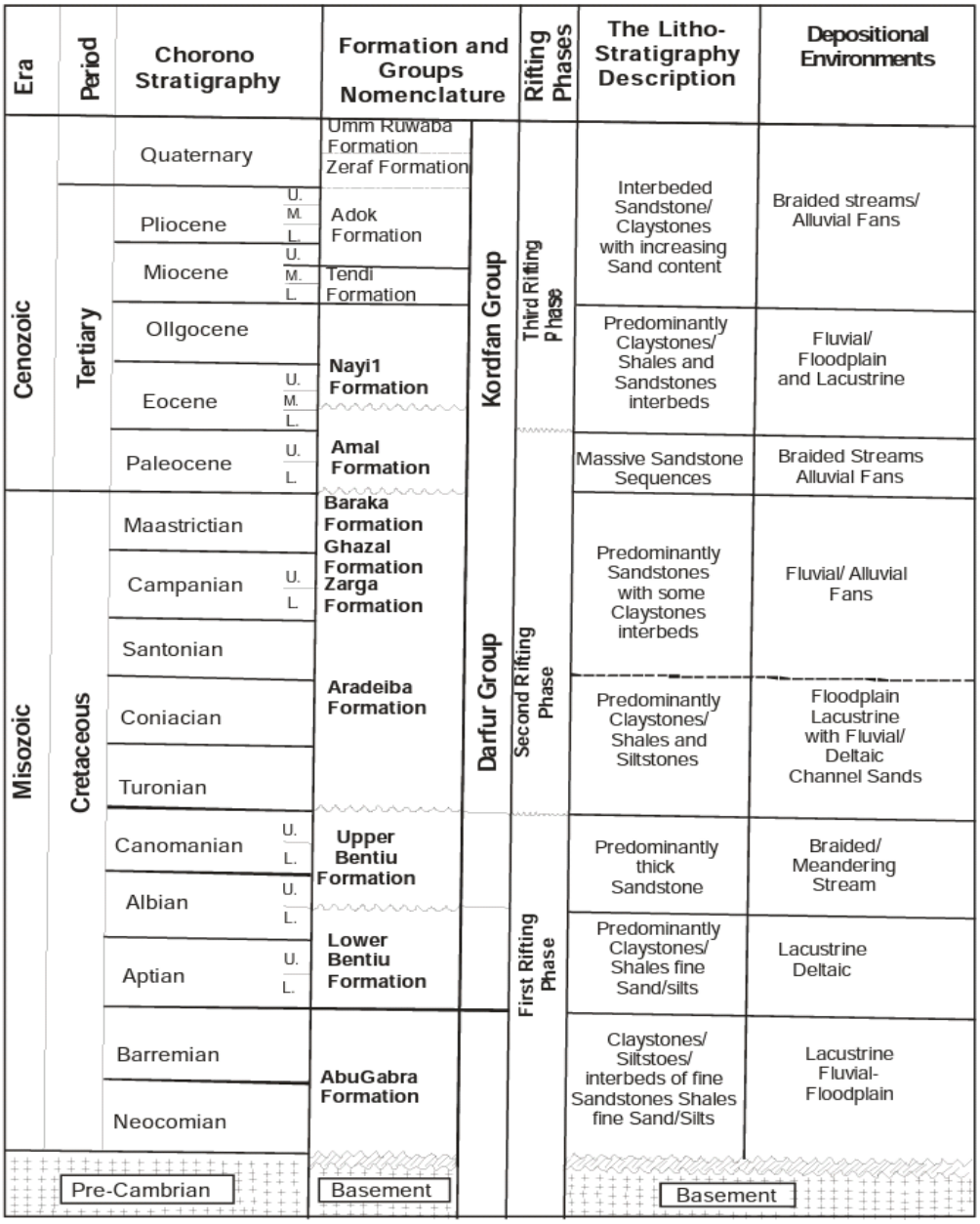


## 2.3.1 Abu Gabra Formation (Neocomian-Berremian):

It consists of organic rich fluvial lacustrine claystones and shales were deposited with interbedded fine-grained sands and silts. The nature of this deposit was probably the result of the humid climate and lack of external drainage, indicating that the basins were tectonically silled. Thickness varies from 1000 to more than 6000 ft (1,829m, Schull, 1988). The basal contact to Lower Abu Gabra Formation is gradational, while the upper contact towards Bentiu Formation is well defined marking a clear break in a sedimentary pattern (Moniem, et al. 1984). Several wells

have recovered oil from sand within this sequence. According to (Schull these sands were deposited in a lacustrine - deltaic environment.

### 2.3.2 Bentiu Formation (Aptian-Cenomanian):

The Bentiu Formation comprises a massive sandstone sequence with some thin claystone interbedded. The claystone grade downwards from reddish brown to medium grey. They are medium to coarse grain and less consolidated than the overlying formation. The claystone appear to have limited lateral continuity, (Moniem, et al. op. cit.). The alluvial and fluvial-floodplain environment expanded probably due to a change from internal to external drainage. The regional basal level, which was created by the earlier rifting and subsidence, no longer existed. These thick sandstone sequences were deposited in braided and meandering streams. They are widely distributed throughout the Muglad basin. This unit, which is up to 5,000ft (1,524m) thick, typically shows good reservoir quality. Sandstones of Bentiu Formation are the primary reservoirs in Unity- and Heglig–fields (Schull, 1988).

### 2.3.3 Darfur Group (Turonian-Maastrichian):

According to the RRI (1990) the Darfur group (DG) has been classified into two more sub groups, namely the Darfur Group Undifferentiated (DGU) with an age extending from the Turonian to Lower Campanian. The Darfur Group Undifferentiated (DGU) has been recognized in the NW of the Muglad Basin. Generally, the Darfur Group comprises the Aradeiba –Zarqa –Ghazal and Baraka Formations. Only in Unity and Heglig areas subdivision into four units can be made. In northwestern Muglad the Darfur Group is reduced to a thin sequence of mostly claystone which cannot be s subdivided further; the tops and bottoms being recognized regionally as unconformities. (Moniem, et al. op. cit.). A brief description of the Darfur Group (DG) is given below:

#### 2.3.3.1 Aradeiba Formation(Turonian-Satonian):

This formation consists of interbedded the floodplain and lacustrine claystone, shales, and siltstones are fluvial /deltaic channel sands.. The thickness varies from 700ft to over 2000ft. The Aradieba sands are important reservoirs in Unity and Heglig field (Schull, op. cit.).

### 2.3.3.2 Zarga Formation(Campanian-Maastrichtian):

This consists of interbedded sandstones and claystone, the relative amount of the sands in this formation is higher than that in Aradeiba Formation. The sandstones are well defined in Unity field. The thickness ranges from 150ft to over 1000ft. (Moniem, et al. op. cit).

### 2.3.3.3 Ghazal Formation (Campanian-Maastrichtian):

This formation consists of interbedded sandstones and claystone similar in composition to sediment assigned to the Zarga Formation. The thicker sands of Ghazal Formation indicate depositional environments of braided streams. The upper Ghazal sandstones indicate a return to the same depositional environment as that of Aradieba and Zarga Formations (Schull, 1988).

### 2.3.3.4 Baraka Formation (Maastrichtian):

This formation consists of sandstones within thin interbedded silty, claystone deposited in fluvial and alluvial fan environments which prograde from the basin margins (Schull, op.cit).

## 2.4 Tertiary Sedimentary Units:

The Tertiary is represented by cropping out sequences of unconsolidated sand, gravels silts and clays deposited in alluvial, fluvial, and shallow lacustrine environments (Vail, 1978). An exposed thick sequence of medium- to coarse grain sediments is associated with the final rifting phase.

### 2.4.1 Amal Formation (Paleocene):

This formation consists of massive sandstones composed dominantly of coarse to medium grain quartz arenites (Schull, op.cit).

### 2.4.2 Kordofan Group (Late Eocene- Quaterary):

The sediments of this group are characterized by the coarsening upward sequences. The lower portion of this group is Nayil and Tendi Formations which are characterized by fine-grain sediments related to the final rifting phase. While the upper section is formed by Adok and Zeraf Formations which is consist of sand and sandstones. The lake deposit of this interval appears to have only minor oil source potential (Shull, 1988). However, they offer an excellent potential as a seal overlying the massive sandstones of the Amal Formation.

### 2.4.2.1 Nayil Formation (late Eocene-Early Oligocene):

This formation represents the lower part of Kordofan Group. It consists of claystone, often silty, interbedded with sandstone. It is mainly distributed in the Kaikang trough. The upper boundary of this formation is taken at the change to the more radioactive clay stones of the Tendi Formation which is often darker in color (RRI, 1990).

### 2.4.2.2 Tendi Formation (late Oligocene -Early Miocene):

This term was previously established by Chevron. Lithologically the formation consists of claystone which locally grade into sub-fissile and fissile shale, trace pyrite, kaolinites and some carbonaceous debris. The boundary is taken at the upward change from the claystone and shale sequence of the Tendi Formation, into the more arenaceous sequence of sand/sandstone and minor claystone of Adok Formation.

### 2.4.2.3 Adok Formation (late Miocene - Pliocene ):

The term Adok Formation was also introduced by Chevron. It consists of sand and sandstones in the variable colour. The formation is widely recognized throughout Muglad Rift Basin. The upper boundary is taken at the upward passage into a clear, more massive sequence of sands and sandstones of the Zeraf Formation.

### 2.4.2.4 Zaraf Formation (Quaternary):

The term Zeraf Formation was given previously by Chevron. It consists of massive sands with variable grain size, but predominantly coarse to very coarse grain. The upper boundary is difficult to be recognized, but generally the formation is widely known throughout Muglad Rift Basin.

# CHAPTER THREE

# LITERATURE REVIEW AND METHODS OF INVESTIGATION

# 3 Literature Review and Methods of Investigation

## 3.1 Historical background of oil and gas exploration in Sudan

Oil exploration in Sudan started in 1959, when Italy's Agip oil company was granted concessions in the Red Sea area, carrying out seismic surveys and drilling six wells. Following Agip into the Red Sea, France's Total, Texas Eastern, Union Texas and Chevron. All yielded nothing for the next fifteen years.

The only successful results were achieved by Chevron in 1974, 120 km southeast of Port Sudan, where dry gas and gas condensate were found at Basha'ir-1 and Suakin-1 wells. Chevron estimated possible production of 50m cubic feet of dry gas and one thousand barrels of gas condensate per day. No oil was found, however, and most companies relinquished their concessions in the region. Since 1991 the main holder of the Red Sea concession has been IPC (International Petroleum Corporation, now part of the Swedish Lundin group).

Exploration for oil in southern and southwestern Sudan began in 1975, when the government of Sudan granted Chevron a concession area of 516,000$km^2$ in blocks around Muglad and Melut. Chevron started geological and geophysical surveys in 1976, and drilled its first well in 1977, which was dry. In 1979, Chevron made its first oil discovery in Abu Jabra #1, west of Muglad, where an 8 million barrels reserve and a 1,000 barrels per day (b/d) production rate were estimated.

In 1997, Greater Nile Petroleum Operating Co. Ltd (GNOPC), a consortium composed of China National Petroleum Corporation (CNPC), Petronas, Oil and Natural Gas Corporation (ONGC) and Sudapet; acquired Blocks 1, 2 and 4 from State Petroleum and launched an extensive exploration and development program. This led to discovery of 1.0 billion barrels of additional reserves. Shortly, GNPOC initiated numerous Field Development Plans (FDPs), constructed 1610 km export pipeline, and eventually, exported the first Sudanese oil in 1999. The pipeline was built in order to transport the crude oil from the fields to the refinery in Khartoum, and then to Bashair in Eastern Sudan.

## 3.2 Methods of Investigation

The interpretation of wire line logs as subsurface techniques is now widely used in Lithology identification and formation properties. A wide range of physical parameters can be measured using tools lowered down a petroleum exploration hole. These give information on lithology, porosity and oil and water saturation (Cant 1984; Allen and Allen 1990; Emery and Myers 1996). In this study the gamma-ray, sonic, spontaneous potential (SP), density, neutron, caliper and focused resistivity wire line logs from the Kiakang 1,2 and 3 were interpreted to identify the lithology and measured formation parameters.

### 3.2.1 Porosity Logs

Although each produces a porosity value from basic measurement none actually measures porosity directly. Two such logs, the density and neutron, are nuclear measurements. A third log, the sonic log, uses acoustic measurements, and the fourth and the newest log senses the magnetic resonance of formation nuclei. When used individually, each of the first three has a response to lithology which must be accounted for, but when used in concert, two or three at a time, lithology can be estimated and a more accurate porosity derived.

#### 3.2.1.1 Sonic Log:

The sonic log is a porosity log that measures interval transit time (Δt) of a compressional sound wave traveling through the formation along the axis of the borehole. The sonic log device consists of one or more ultrasonic transmitter and two or more receivers. Modern sonic logs are borehole-compensated (BHC) devices. These devices are designed to greatly reduce the spurious effects of borehole size variations as well as errors due to tilt of the tool with respect to the borehole axis by averaging signals from different transmitter-receiver combinations over the same length of borehole.

Interval transit time (Δt) in microseconds per foot, μsec/ft (or microsecond per meter. μsec/m) are the reciprocal of the velocity of a compressional sound wave in feet per second (or meters per second). The interval transit time (Δt) is dependent upon both lithology and porosity. Therefore a formation's matrix interval time must be known to derive sonic porosity by the following formulas:

Wyllie time-average equation:

$$\emptyset \mathbf{s} = [(\Delta \mathbf{t}\,\mathbf{log} - \Delta \mathbf{t}\,\mathbf{ma})/(\Delta \mathbf{t}\,\mathbf{fl} - \Delta \mathbf{t}\,\mathbf{ma})]$$

Raymer-Hunt-Gardner (RHG):

$$\emptyset \mathbf{s} = \frac{\mathbf{5}}{\mathbf{8}} \left[ (\Delta \mathbf{t\,log} - \Delta \mathbf{t\,ma}) / \Delta \mathbf{t\,log} \right]$$

Where:

Øs= sonic-derived porosity

Δt ma =interval transit time in the matrix

Δt log =interval transit time in the formation

Δt fl = interval transit time in the fluid in the formation (freshwater mud = 189 μsec/ft salt water mud = 185 μsec/ft).

### 3.2.1.1.1 Hydrocarbon Effect

The interval transit time (**Δt**) of a formation is increased due to the presence of hydrocarbons (i.e., hydrocarbon effect). If the effect of hydrocarbons is not corrected, the sonic-derived porosity is too high. Hilchie suggests the following empirical corrections for hydrogen effect:

$$\phi = \phi s \times 0.7 \quad \text{(gas)}$$
$$\phi = \phi s \times 0.9 \quad \text{(oil)}$$

### 3.2.1.2 Density Log

Density is measured in (**g/cm$^3$** or K **g/m$^3$**) and is indicated by the Greek later ρ (roh). Two separate density value are used by the density log; the bulk density (**ρb**) and the matrix density (**ρma**). The bulk density is the density of entire formation (solid and fluid parts) as measure by the logging tool. The matrix density is the density of the solid framework of the rock.

The density logging tool has a relatively shallow depth of investigation, and as result, is held against the side of the borehole during logging to maximize its response to the formation. The tools are comprised of a medium-energy gamma ray source. Two gamma ray detectors provide some measure of compensation for borehole conditions.

When the emitted gamma rays collide with the electrons in the formation, the collisions result in a loss of energy from the gamma ray particle. The scattered gamma rays that return to the detectors in the tool are measured in two energy ranges. The number of returning gamma rays in the higher energy range, affected by Compton

scattering, is proportional to the electron density of the formation. Gamma ray interactions in the lower energy range are governed by the photoelectric effect. The response from this energy range is strongly dependent on lithology and only very slightly dependent on porosity.

Formation bulk density (**ρb**) is a function of matrix density, porosity, and density of the fluid in the pores (saltwater mud, freshwater mud, or hydrocarbons). To determine density porosity either by chart or by calculation, the matrix density and type of the fluid in the formation must be known. The formula for calculating density porosity is:

$$\emptyset \mathbf{D} = \frac{\boldsymbol{\rho ma - \rho b}}{\boldsymbol{\rho ma - \rho f}}$$

Where:

ØD = density derived porosity

ρma = matrix density

ρb = formation bulk density

ρfl= fluid density.

### 3.2.1.2.1 Hydrocarbon Effect

Where invasion of a formation is shallow, the low density of the formations hydrocarbons causes the calculated density porosity to be greater than the actual porosity. Oil does not significantly affect density porosity, but gas does (gas effect). Hilchie suggests using a gas density of 0.7 g/cm$^3$ for fluid density (ρfl) in the density porosity formula if gas density is unknown. Because the presence of oil has little effect on the density log, this tool usually provides the best indication of porosity in liquid-filled holes.

### 3.2.1.3 Neutron Log

Neutron log is one of porosity logs that measure the hydrogen concentration in a formation. In clean formation (i.e., shale free) where the porosity is filled with water or oil, the neutron log measure liquid-filled porosity (ΦN).

Neutrons are created from a chemical source in the neutron logging tool. The chemical source is usually a mixture of americium and beryllium which continuously emit neutrons. When these neutrons collide with the nuclei of the formation the

neutron loses some of its energy. With enough collisions the neutron is absorbed by a nucleus and a gamma ray is emitted. Because the hydrogen atom is almost equal in mass to the neutron, maximum energy loss occurs when the neutron collides with the hydrogen atom. Therefore, the energy loss is dominated by the formations hydrogen concentration. Because hydrogen in a porous formation is concentrated in the fluid-filled pores, energy loss can be related to the formations porosity.

Neutron log response varies, depending on:

- Differences in detector types and what are they detect (gamma rays and / or neutrons of different energies).
- Spacing between source and detector.
- Lithology (i.e., sandstone, limestone, and dolomite).

It should be noted that the neutron log response is inversely proportional to porosity so that low-measurement unit values correspond to high porosities, and high measurement unit values correspond to low porosities.

The first modern neutron log (where porosity was directly displayed) was the sidewall neutron log. Like the density log (and for the same reason of limited depth of investigation), the sidewall neutron log has both the source and detector in a pad that is pushed against the side of the borehole. Although the sidewall neutron log was relatively insensitive to lithologic effects, it was sensitive to borehole effects, such as rugosity (roughness) which caused measurement difficulties.

The most commonly used neutron log is the compensated neutron log which has a neutron source and two detectors. Like the sidewall neutron log, it directly displayed values of porosity. The advantage of compensated neutron logs over sidewall neutron logs is that they are less affected by borehole irregularities. Both the sidewall and compensated neutron logs can be recorded in apparent limestone, sandstone, or dolomite porosity units.

#### 3.2.1.3.1 Hydrocarbon Effect

Whenever pores are filled with gas rather than oil or water, the reported neutron porosity is less than the actual formation porosity. This occurs because there is a lower concentration of hydrogen in gas rather than in oil or water. This lower concentration is not accounted for by the processing software of the logging tool, and

thus is interpreted as low porosity. A decrease in neutron porosity by the presence of gas called gas effect.

#### 3.2.1.3.2 Shale Effect

Whenever clays are part of the formation matrix, the reported neutron porosity is greater than the actual formation porosity. This occurs because the hydrogen that is within the clays structure and in the water bound to the clay is sensed in addition to the hydrogen in the pore space. Because the processing software of the logging tool expects all hydrogen in the formation to reside in the pores, the extra hydrogen is interpreted as been part of the porosity. An increase in neutron porosity by the presence of clay is called shale effect.

Table 3-1: showing the comparison between the Porosity logs

| | **Advantages** | **Limitations** |
|---|---|---|
| **Neutron density** | Given two possible lithology pair solutions, the porosity remains relatively invariant between solutions.<br>The combination of neutron and density is the most common of all porosity tool pair. | In rough holes or in heavy drilling muds, the density data might be invalid. |
| **Neutron sonic** | Given two possible lithology pair solutions, the porosity remains relatively invariant between solutions.<br>The sonic is less sensitive to rough holes than the density. | The combination of sonic and neutron data (without the density) is not common. |
| **Spectral density (bulk density)** | Both measurements are made with the same logging tool; both will be available in newer wells. | The choice of lithology pair will have a significant effect of the estimation of porosity. In rough holes or in heavy drilling mud, the data may be invalid. |
| **Sonic density** | Best for identifying radioactive reservoirs , rather than predicting lithology and porosity:<br>Potential reservoirs plot along the closely spaced lithology lines while shale tend to fall toward the lower right of the plot.<br>This can indicate the presence of radioactive reservoirs which are intermingled with the shale (which tend to have high radioactivity). | The choice of lithology pair has a significant effect on the estimation of porosity.<br>The lithology line is closely spaced, so any uncertainty in the measurements produces large changes in the lithology and porosity estimates. |

### 3.2.2 Lithology Logs

### 3.2.3 Gamma Ray (GR)

Gama ray logs measured the natural radioactivity in formation and can be used for identifying lithology and for correlation zone.

Shale-free sandstone and carbonate have low concentration of radioactive material and give low gamma ray reading, as shale content increases the gamma ray log response increases because of the concentration of radioactive material in shale, however clean sandstone (i.e. with low shale content) might also produce a high gamma ray response, if the sandstone contains potassium feldspars, micas, glauconite or uranium rich water.

If a zone has a high potassium content coupled with a high gamma ray log response, the zone might not be shale, instead it could be a feldspathic, glauconite or micaceous sandstone, gamma ray logs can be used not only for correlation but also for the determination of shale volumes, the gamma ray response is not affected by formation resistivity (**Rw**), it can be used in cased hole and in open holes containing non-conducting drilling fluids (i.e. oil – based muds or air).

#### 3.2.3.1.1 Operating Principle of Gamma Ray Tools

Traditionally, two types of gamma ray detectors have been used in the logging industry Geiger.

Mueller and scintillation detectors today most gamma ray tools use a sodium iodide (NaI) crystal newer and more efficient crystal materials are constantly being discovered but the principles of operation are the same, when a gamma ray strikes the crystal, a single photon of Light is emitted this tiny flash of light then strikes a photocathode (probably made from cesium antimony or silver-magnesium) each photon hitting the photocathode releases a bunch of electrons.

These in turn are accelerated in an electric field to strike another electrode producing an even bigger "shower of electrons, this process is repeated through a number of stages until a final electrode conducts a small current through a measure resistor to produce a voltage pulse that can be measured.

Each detected gamma ray produces a single pulse , the "dead time of these systems vary but are typically very short, and they can register many counts/second before being "swamped by numerous near-simultaneous gamma rays.

### 3.2.3.1.2 The interpretation of gamma ray logs can be summarized as follows

In a given area, only the relative radioactivity of the various rocks is of significance.Rocks of low radioactivity includes primarily clean sands, sandstones, limestones, and dolomites. Anhydrite, salt, lignite and coal have also a low radioactivity, their radioactivity increases when they are shaly.Ordinary shales have a much higher radioactivity than the rocks listed above, the radioactivity of sandy shales is less than that of shales, and shales are sufficiently high in radioactivity and can generally be easily distinguished from the other rocks on a gamma ray log.

### 3.2.3.1.3 Shale Volume Calculation

Because shale is usually more radioactive than sand or carbonate, gamma ray logs can be used to calculate volume of shale in porous reservoir, calculation of the gamma ray index is the first step needed to determine the volume of shale from a gamma ray log:

$$IGR = \frac{GRlog - GRmin}{GRmax - GRmin}$$

**Where:**

IGR = gamma ray index.

GRlog = gamma ray reading of formation.

GRmin = minimum gamma ray (clean sand or carbonate).

GRmax = maximum gamma ray (shale).

### 3.2.3.1.4 Spectral Gamma ray log

The spectral gamma ray log record not only the number of gamma rays emitted by the information but also the energy of each and processes that information into curves representative of the amount of thorium (**Th**), potassium (**K**), and uranium (**U**) present in the formation.

### 3.2.3.1.5 Important uses of the spectral gamma ray log include (dresser – atlas, 1981)

i. Determining shale (clay) volume (V. Shale) in sandstone reservoir that contains uranium minerals, potassium feldspars, micas and / or glauconite.
ii. Differentiating radioactive reservoir from shale.
iii. Source – rock evaluation.
iv. Evaluation of potash deposits.
v. Geologic correlation.
vi. Clay typing.
vii. Fracture detection.
viii. Rock typing in crystalline basement rocks.

### 3.2.3.1.6 Advantage of Gamma Ray Log (GR)

An advantage of the gamma log over some other types of well logs is that it works through the steel and cement walls of cased boreholes although concrete and steel absorb some of the gamma radiation, enough travels through the steel and cement to allow qualitative determinations.

Sometimes non-shales also have elevated levels of gamma radiation, sandstone can contain uranium mineralization, potassium feldspar, clay filling, or rock fragments that cause it to have higher-than usual gamma readings coal and dolomite may contain absorbed uranium evaporate deposits may contain potassium minerals such as carnallite, when this is the case, spectral gamma ray logging can be done to identify these anomaly.

### 3.2.3.2 Spontaneous Potential (SP)

The SP response of shale is relatively constant and follows a straight line called a shale baseline, the (**SP**) value of the shale baseline is assumed to be zero , and SP curve deflection are measured from this baseline permeable zones are indicated where there SP deflection from the shale baseline.

The magnitude of SP deflection is due to the difference in salinity between mud filtrate and formation water, and not to the amount of permeability this salinity difference produces a difference in the resistivity of the mud filtrate (Rmf) and formation water (Rw), it is important to remember that normally the SP curve has less deflection in hydrocarbon – bearing zones.

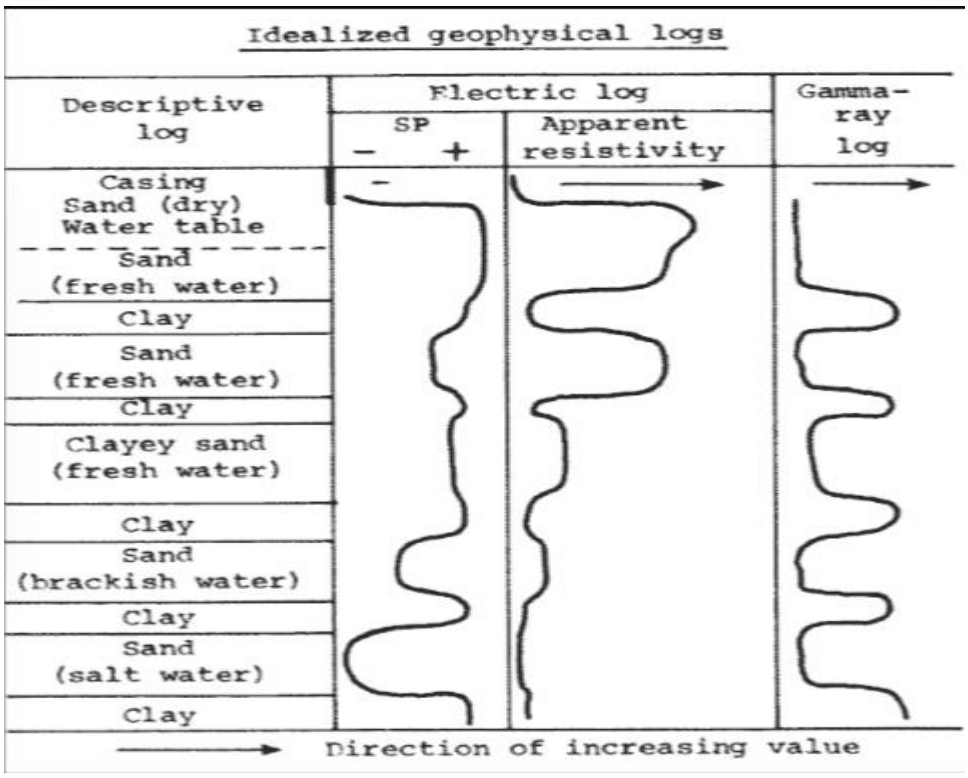


3.1 Figure: Figure: simplified interpretation of SP log3

The SP log can be used to calculate the volume of shale in a permeable zone by the following formula:

**V. Shale = 1.0 – (PSP / SSP)**

**Where:**

V. Shale = volume of shale.

PSP = pseudo-static spontaneous potential (maximum SP of shaly formation).

SSP = static spontaneous potential of a nearby tick clean sand.

OR, alternately:

V. Shale = (PSP – SSP) / (SP Shale – SSP)

**Where:**

SP Shale = value of SP in a shale (usually assumed to be zero).

Also the SP log can be used to detect permeable beds and boundaries of permeable beds; the SP has the following responses relative to the shale baseline:

Negative deflection (to the left of the shale baseline) where:

**Rmf > Rw**

Positive deflection (to the right of the shale baseline) where:

**Rmf < Rw**

No deflection where:

**Rmf =Rw**

The SP response can be suppressed by thin beds shaleness and the presence of hydrocarbons.

#### 3.2.3.2.1 Advantage of SP Log

if the well is losing water the SP curve can be used to pinpoint the water lose point, the SP system will detect the electro-filtration potential generated by the moving water this should be run with and compared to the gamma ray curve, this can easily be done because the two curves resemble each other thus the anomalous zone on the SP will be easier to spot.

#### 3.2.3.2.2 Limitations of SP Log

i. The SP cannot be recorded in air or oil-base muds, since there is no conductive fluid in the borehole.
ii. If the resistivity of formation water equals the resistivity of the mud filtrate, there is no SP.
iii. Conductive mud is essential for generation of a spontaneous potential.
iv. In salt-mud, SP tends to be straight line (less salinity contrast).
v. If bed is too thin, the full SP will not develop. Chart exist to correct for this effect, but only significant for bed thickness <20ft.
vi. Hydrocarbon and shale in the formation reduce SP development.

## 3.3 Resistivity Logs

Is the electric property that impedes a current? A current flowing through a wire (or resistor) is like water flowing through a pipe, and the voltage drop across the wire is like pressure drop which pushes water through the pipe.

Resistance is proportional to how much pressure is required to achieve a given flow, while conductance is proportional to how much flow occurs for a given pressure. Conductance and resistance are reciprocals. The resistance of an object depends on its shape and the material of which it is composed. The resistivity of different materials varies by an enormous amount. The resistivity measured by ohm-meter (**Ω-m**).

Generally resistivity logs are used to:

- Determine hydrocarbon-bearing versus water bearing zone.
- Indicate permeability zones.
- Determine porosity.

The most important use of resistivity logs is the determination of hydrocarbon-bearing versus water-bearing zones. Because the rock's matrix or grains are nonconductive and any hydrocarbons in the pores are also nonconductive, the ability of the rock to transmit a current is almost entirely a function of water in the pore .as the hydrocarbon saturation of the pores increases (as the water saturation decreases), the formation's resistivity increases. as the salinity of the water in pores decreases (as Rw increases) the rock resistivity also increases .a geologist by knowing several parameters (a,m,n and Rw), and by determining from logs the porosity (phi)and the formation bulk ,or true resistivity (**Rt**) ,can determine the formation's water saturation (Sw) from the Archie equation:

$$\mathbf{Sw} = \left(\frac{\mathbf{Rw} * \mathbf{a}}{\mathbf{Rt} * \mathbf{phi^m}}\right)^{\frac{1}{n}}$$

Resistivity logs produce a current in the adjacent formation and measure the response the response of the formation to that current .the current can be produced and measured by either of two methods .electrodes tools (also called galvanic devices or, for presently available versions, laterologs) .Induction tools use coils to induce a current and measure the formation's conductivity. These two types of tools have many variations which are summarized in table (1). In many cases, it is desirable to use both of electrode and induction tools to produce a single resistivity log

Table 3-2: Difference between resistivity log tools

| | | |
|---|---|---|
| Induction logs (coil log) (measure formation conductivity) | | |
| Induction (deep and medium) | | |
| Galvanic device ( electrode logs and laterologs ) (measure formation resistivity ) | | |
| Normal | Microlaterolog (**MLL**) | |
| Lateral | Microlog (**ML**) | |
| Laterolog (deep and shallow) | Proximity Log (**PM**) | |
| Spherical focused log (**SFL**) | Microspherically focused log (**MSFL**) | |
| Resistivity log depth of investigation | | |
| Flushed zone (**Rxo**) | Invaded zone (**Ri**) | Uninvaded zone (**Rt**) |
| Microlog (**ML**) | Short normal (**SN**) | Long normal (**LN**) |
| Microlaterolog (**MLL**) | Laterolog-8 (**LL8**) | Lateral log |
| Proximity Log (**PM**) | Spherical focused log (**SFL**) | Deep induction log (**DIL**) |
| Microspherically focus Log (**MSFL**) | Medium induction log (**ILm**) | Deep laterolog (**DLL**) |
| | Shallow laterolog (**LLs**) | Laterolog-3 (**LL3**) |
| | | Laterolog-7 (**LL7**) |

### 3.3.1 Latrologs

Electrode logs are designed to measure formation resistivity in borehole filled with saltwater mud (where Rmf ~ Rw ) a current from surveying electrode is forced into formation by focusing electrodes .focusing electrodes (guard electrodes) emits current of same polarity as the surveying electrodes but are located above and below it .and prevent the surveying current from flowing up the borehole filled with saltwater mud .the effective depth of laterologs investigation is controlled by the extent to which the surveying current is focused. Deep reading laterologs are therefore more strongly focused than shallow reading laterologs.

Invasions can influence the laterolog .however because the resistivity of the mud filtrate is approximately equal to resistivity of formation water (Rw~Rmf). The borehole size and formation thickness effect the lterolog, but normally the effect is small enough so that laterolog resistivity can be taken as Rt.

The dual laterolog is modern version of laterologs. It consist of deep-reading measurement (Rlld) and the shallow-reading measurement (Rlls) both curves are

displayed in tracks 2 and 3 of the log. usually on four cycle logarithmic scale ranging from 0.2 to 2000 ohm-m.the third resistivity measurement is the microspherically focused resistivity (Rmsfl) which have a very shallow depth of investigation and measures the formation resistivity very close of wellbore.

### 3.3.2 Induction log

Induction logs measure formation conductivity rather than resistivity .formation conductivity is related to formation resistivity through the following equation:

$$C = \frac{1000}{R}$$

Where:

C=conductivity in milimho/m (=milisiemens)

R=resistivity in ohm-m

An induction tool consist of several transmitting coils that emits a high-frequency alternating current of constant intensity. Which create electromagnetic field that's induce signals in receiver coils. The response of the individual coils are combined in such a way as to minimize the effect of materials in borehole

By design, induction logs work well in wells containing non-conducting fluids in the borehole. Also have a different generation like; induction electric log (first version) and dual induction log.

### 3.3.3 Flushed Zone Resistivity Logs

Another class of tools based on the same physical principles was being designed expressly to interrogate the region very close to borehole. This region usually flushed by the drilling mud. The tool must make good contact with the borehole wall for a valid measurement, and a thick mud cake or a rough hole adversely affected the measurement.

### 3.3.4 Micro log (ML)

The microlog is a pad-type resistivity device that primary detects mud cake. The pad is in contact with borehole and consist of three electrodes spaced one inch apart. The two resistivity measurements are made; the micro-normal (**R2**) and the micro-inverse (**R1x**).through the resistivity of mud filtrate (**Rmf**) is less than the

resistivity of mud cake (**Rmc**) the micro-normal curve reads the higher resistivity in permeable zone than the shallower reading micro-inverse curve. The microlog does not work well in saltwater or gypsum-based muds.

### 3.3.5 Interpretation

Porosity the minerals that's make up the grains in the matrix of rock and the hydrocarbons in the pores of rock are nonconductive .therefore, the ability of rock to transmit the electrical current is almost entirely the result of the water in the pore space .thus, resistivity measurements can be used to determine porosity. Normally measurements of a formation's resistivity close to the borehole (flushed zone, Rxo or invaded zone Ri) are used to determine porosity.

When a porous, permeable, water-bearing formation the porosity (**Φ**):

$$\mathbf{\Phi = \left(\frac{Rmf * a}{Rxo}\right)^{1/m}}$$

Where:

Rmf= resistivity of mud filtrate at formation temperature

Rox= flushed zone resistivity

a= tortuosity factor

m=cementation exponent

In a hydrocarbon-bearing zones

$$\mathbf{\Phi = \left[\frac{a * Rmf}{Sxo^2 * Rxo}\right]^{1/m}}$$

Where:

Sox=flushed zone water saturation =1.0 – RHS (residual hydrocarbon saturation)

By far the most important use of resistivity log is the determination of hydrocarbon-bearing versus water bearing zones. Because the rocks matrix or grain are nonconductive and any hydrocarbons in the pores are also nonconductive, the ability of the rock to transmit a current is almost entirely a function of water in the pores. As the hydrocarbon saturation of the pores increase (as the water saturation decreases), the formations resistivity increases. As the salinity of the water in the pores decreases (as Rw increases), the rock resistivity also increases.

# CHAPTER FOUR

# RESULTS AND DISCUSSION

# 4 Results and discussion

## 4.1 Calculation

### 4.1.1 Lithology logs

By using gamma ray log we distinguish shale zones from sand zones and calculate the shale volume in sand zones traced the following steps:

First: determine from logs sand baseline (minimum GR value) and shale baseline (maximum GR value), then compute the cut off by the following equation:

$$cutoff = \frac{\min GRvalue + \max GRvalue}{2}$$

Second: any values less than cut off are considered sand zones .whereas values greater than cut off are shale zones.

Third: in the sand zones we read average value which used to calculate gamma ray index (**IGR**):

$$IGR = \frac{GRlog - GRmin}{GRmax - GRmin}$$

Then calculated the shale volume (**Vsh**) by the following equation:

$$Vsh = 0.33 * (2^{(2*IGR)} - 1)$$

### 4.1.2 Porosity logs

- Density log:

The equation that has been used to calculate density porosity expressed by:

$$\phi = \frac{\rho_{ma} - \rho_b}{\rho_{ma} - \rho_f}$$

Where:

ρma = density of matrix ( 2.65 g/cm$^3$).

ρf = density of fluid ( 1 g/cm$^3$).

ρb = density of bulk (it's obtained from the density log for different sand zones).

- Neutron log:

The neutron porosity has been directly measured from the neutron log for different sand zones.

- Sonic log:

The equation that has been used to calculate sonic porosity expressed by:

$$\Phi = \frac{\Delta t \log - \Delta t\ mat}{\Delta t\ f - \Delta t\ mat}$$

Where:

Δt log = interval transit time (it's obtained from log for different sand zones).

Δt mat = interval transit time of the matrix (55.5 msec).

Δt f = interval transit time of the fluid (189 msec).

After that has been calculated the average of porosity for three values by the following equation:-

$$\Phi avg = \frac{\Phi\text{sonic} + \Phi\text{density} + \Phi\text{neutron}}{3}$$

### 4.1.3 Resistivity logs

We are reading from log the values of deep latero log resistivity (**RLLD**), shallow latero log resistivity (**RLLS**) and micro spherically focus log (**Rmsfl**).then correct the deep and shallow latero log resistivity for:

1-Borehole conditions: using flowing chart

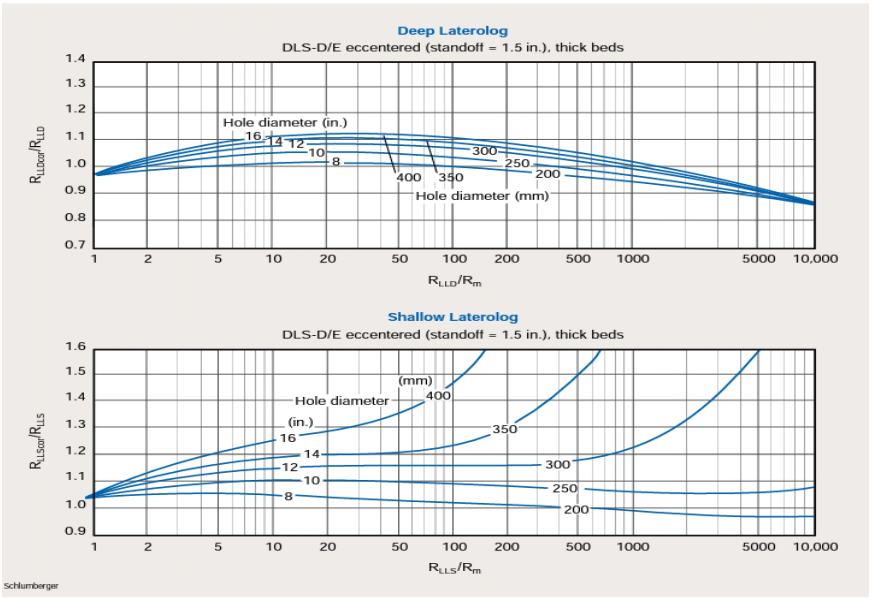


4.1 Figure: borehole correction chart

2-bed thickness: using flowing chart

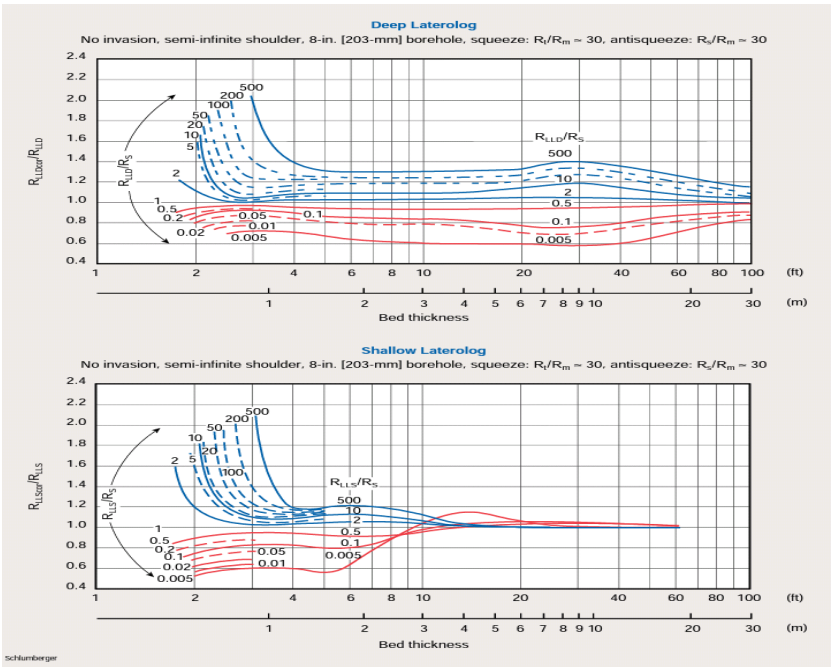


4.2 Figure: bed thickness correction chart

Also correct micro spherically focus resistivity for mud cake effect by using the flowing chart:

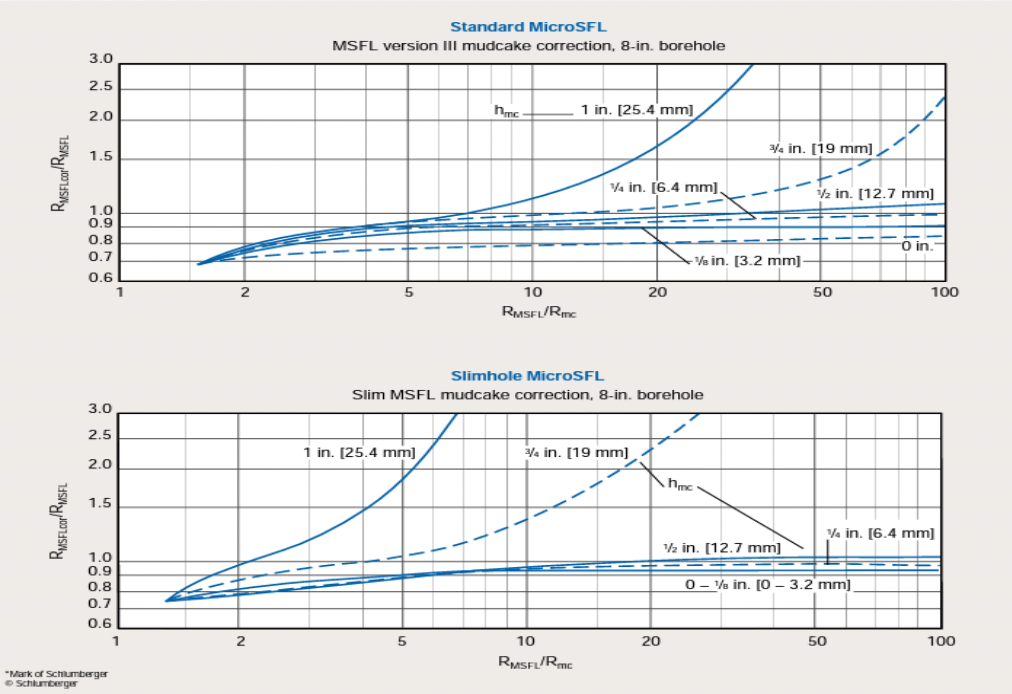


4.3 Figure : invasion correction chart.

In all above correction we depend on some values from header information's such as:

Resistivity of drilling mud (Rm=0.9Ω.m)

Resistivity of mud cake (Rmc=0.125)

Hole diameter (h=10in)

Thick of mud cake (Hmc=0.25in)

Then we calculate the true resistivity (Rt) using flowing chart

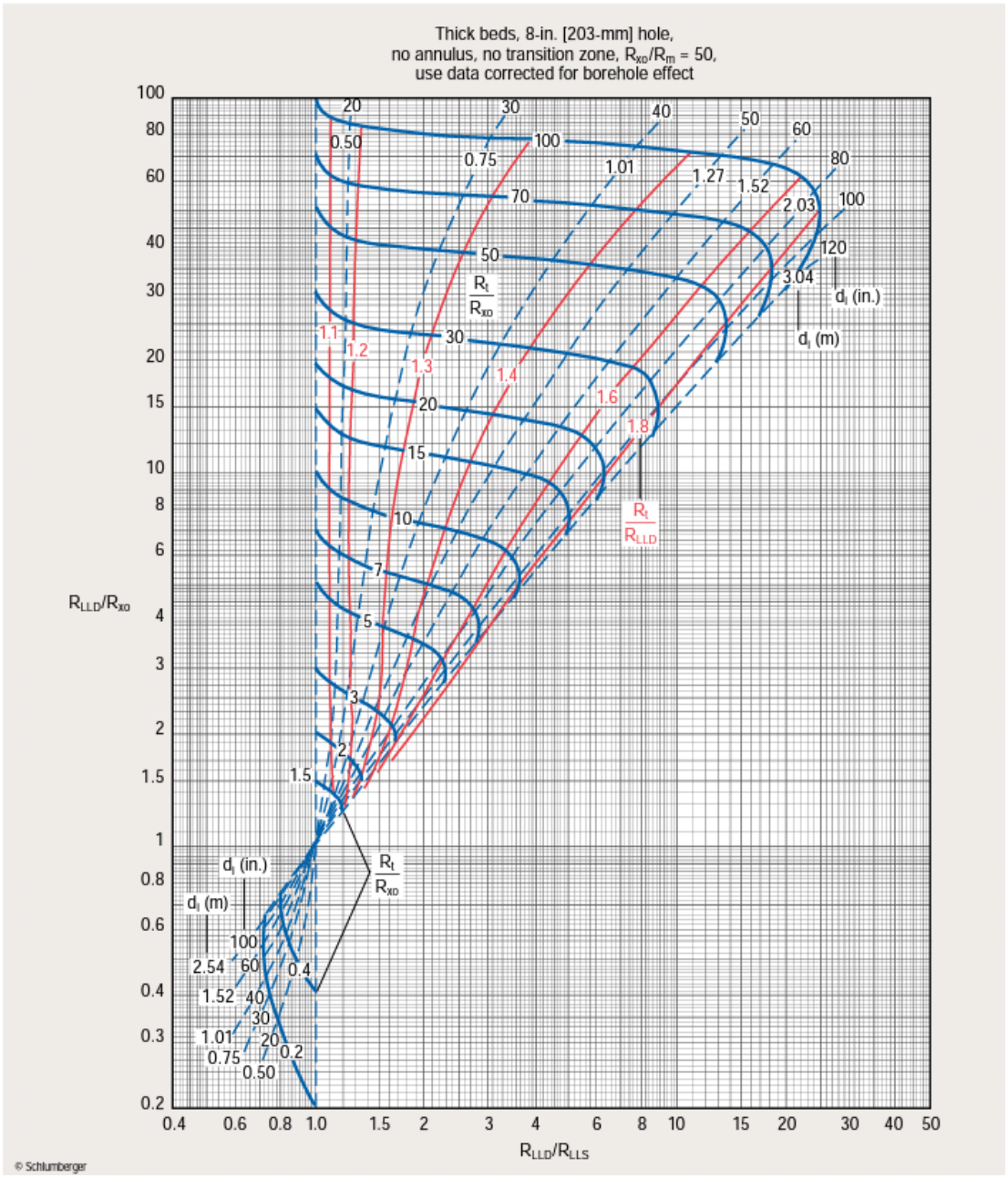


4.4 Figure : : true resistivity chart

Finally we calculated the water saturation (Sw) by flowing equation:

$$Sw = \sqrt{\frac{Ro}{Rt}}$$

Where:

Ro [is constant refer to deep induction resistivity measured in clean sand zones filled 100% water saturation [(0.55Ω-m)].

**Rt** is true resistivity of the formation.

Notice that all above calculation are done by using excel sheet illuminated below

Table 4.1: portion of Excel sheet calculation for kaikange well-1

| POROSITY logs | | | | | | | |
|---|---|---|---|---|---|---|---|
| Φ Avg | ΦN | ΦD | Pb | Φ S | Δt | Depth | formation thickness |
| 38.71286 | 27 | 33.33333 | 2.1 | 55.80524 | 130 | 1250 | 1.5 |
| 36.98994 | 31 | 35.40052 | 2.1 | 44.56929 | 115 | 1253 | 1 |
| 30.91357 | 26 | 24.4186 | 2.27 | 42.3221 | 112 | 1255 | 1 |
| 18.11401 | 21 | 22.48062 | 2.3 | 10.86142 | 70 | 1257 | 5.5 |
| 34.42663 | 33 | 25.71059 | 2.25 | 44.56929 | 115 | 1284 | 1 |
| 37.55104 | 27 | 37.3385 | 2.07 | 48.31461 | 120 | 1293 | 1 |
| 40.56148 | 39 | 41.86047 | 2 | 40.82397 | 110 | 1297 | 2 |
| 31.18642 | 34 | 22.48062 | 2.3 | 37.07865 | 105 | 1302 | 0.8 |
| 32.00641 | 30 | 28.94057 | 2.2 | 37.07865 | 105 | 1304 | 2 |
| 31.83463 | 30 | 32.17054 | 2.15 | 33.33333 | 100 | 1306 | 2.5 |
| 29.83463 | 24 | 32.17054 | 2.15 | 33.33333 | 100 | 1311 | 6.7 |
| 34.25485 | 33 | 28.94057 | 2.2 | 40.82397 | 110 | 1320 | 0.5 |
| 30.75797 | 30 | 28.94057 | 2.2 | 33.33333 | 100 | 1322 | 1.3 |
| 29.68131 | 30 | 25.71059 | 2.25 | 33.33333 | 100 | 1324 | 1 |
| 29.75797 | 27 | 28.94057 | 2.2 | 33.33333 | 100 | 1328 | 2 |
| 30.75797 | 30 | 28.94057 | 2.2 | 33.33333 | 100 | 1331 | 4.2 |
| 29.75797 | 27 | 28.94057 | 2.2 | 33.33333 | 100 | 1336 | 20 |
| 32.91128 | 30 | 35.40052 | 2.1 | 33.33333 | 100 | 1356 | 1.2 |
| 30.68131 | 33 | 25.71059 | 2.25 | 33.33333 | 100 | 1360 | 3 |
| 29.25734 | 24 | 28.94057 | 2.2 | 34.83146 | 102 | 1364 | 14 |
| 30.75797 | 30 | 28.94057 | 2.2 | 33.33333 | 100 | 1378 | 2.5 |
| 32.16796 | 31 | 32.17054 | 2.15 | 33.33333 | 100 | 1381 | 4.7 |
| 26.53594 | 24 | 23.77261 | 2.28 | 31.83521 | 98 | 1386 | 17 |
| 30.83463 | 27 | 32.17054 | 2.15 | 33.33333 | 100 | 1400 | 3 |
| 30.75797 | 30 | 28.94057 | 2.2 | 33.33333 | 100 | 1405 | 0.8 |
| 26.43287 | 24 | 25.71059 | 2.25 | 29.58801 | 95 | 1409 | 29 |
| 30.92526 | 32 | 28.94057 | 2.2 | 31.83521 | 98 | 1411 | 0.9 |
| 29.75797 | 27 | 28.94057 | 2.2 | 33.33333 | 100 | 1443 | 5 |
| 31.54264 | 33 | 28.29457 | 2.21 | 33.33333 | 100 | 1446 | 0.8 |
| 32.83463 | 33 | 32.17054 | 2.15 | 33.33333 | 100 | 1453 | 2 |
| 28.75797 | 24 | 28.94057 | 2.2 | 33.33333 | 100 | 1458 | 5.5 |
| 31.68131 | 36 | 25.71059 | 2.25 | 33.33333 | 100 | 1464 | 1.9 |
| 30.39602 | 30 | 26.35659 | 2.24 | 34.83146 | 102 | 1475 | 4 |
| 32.79108 | 33 | 28.29457 | 2.21 | 37.07865 | 105 | 1479 | 0.8 |
| 34.01464 | 43 | 25.71059 | 2.25 | 33.33333 | 100 | 1493 | 2 |
| 26.27132 | 23 | 22.48062 | 2.3 | 33.33333 | 100 | 1498 | 2.9 |
| 27.35496 | 27 | 22.48062 | 2.3 | 32.58427 | 99 | 1503 | 2.9 |
| 29.77444 | 41 | 22.48062 | 2.3 | 25.8427 | 90 | 1507 | 0.8 |

Table 4.2: portion of Excel sheet calculation for kaikange well-1

| Resistivity Log | | | lithology log | | |
|---|---|---|---|---|---|
| RLLS | Rlld | Rmsfl | VSH | I | GR log |
| - | 30 | 1 | 0.139537 | 0.254386 | 65 |
| - | 25 | 4 | 0.111838 | 0.210526 | 60 |
| - | 60 | 9 | 0.122716 | 0.22807 | 62 |
| - | 95 | 3 | 0.122716 | 0.22807 | 62 |
| - | 6 | 1.2 | 0.151096 | 0.27193 | 67 |
| - | 8 | 2 | 0.193842 | 0.333333 | 74 |
| - | 10 | 4 | 0.187511 | 0.324561 | 73 |
| - | 12 | 1.4 | 0.175076 | 0.307018 | 71 |
| - | 16 | 0.8 | 0.193842 | 0.333333 | 74 |
| - | 16 | 0.6 | 0.128255 | 0.236842 | 63 |
| - | 60 | 0.8 | 0.145281 | 0.263158 | 66 |
| - | 35 | 0.6 | 0.122716 | 0.22807 | 62 |
| - | 80 | 2 | 0.193842 | 0.333333 | 74 |
| - | 10 | 1.8 | 0.128255 | 0.236842 | 63 |
| - | 16 | 0.8 | 0.117244 | 0.219298 | 61 |
| - | 40 | 0.8 | 0.111838 | 0.210526 | 60 |
| - | 60 | 0.8 | 0.09601 | 0.184211 | 57 |
| - | 30 | 0.4 | 0.156982 | 0.280702 | 68 |
| - | 40 | 0.6 | 0.16294 | 0.289474 | 69 |
| - | 60 | 0.6 | 0.111838 | 0.210526 | 60 |
| - | 40 | 1.8 | 0.111838 | 0.210526 | 60 |
| - | 100 | 0.8 | 0.029321 | 0.061404 | 43 |
| - | 100 | 1.8 | 0.187511 | 0.324561 | 73 |
| | 30 | 2 | 0.085774 | 0.166667 | 55 |
| - | 16 | 0.5 | 0.139537 | 0.254386 | 65 |
| - | 40 | 10 | 0.128255 | 0.236842 | 63 |
| - | 5 | 0.6 | 0.139537 | 0.254386 | 65 |
| - | 18 | 0.6 | 0.128255 | 0.236842 | 63 |
| - | 7 | 0.4 | 0.047231 | 0.096491 | 47 |
| - | 7 | 0.6 | 0.156982 | 0.280702 | 68 |
| - | 15 | 0.8 | 0.145281 | 0.263158 | 66 |
| - | 10 | 3 | 0.181256 | 0.315789 | 72 |
| - | 8 | 0.5 | 0.193842 | 0.333333 | 74 |
| - | 4 | 0.5 | 0.111838 | 0.210526 | 60 |
| - | 4 | 0.4 | 0.117244 | 0.219298 | 61 |
| - | 10 | 0.8 | 0.151096 | 0.27193 | 67 |
| - | 8 | 0.5 | 0.187511 | 0.324561 | 73 |
| - | 5 | 1 | 0.193842 | 0.333333 | 74 |

Table 4.3: Excel sheet calculation for kaikange well-3

| porosity logs | | | | | | Depth | formation thickness |
|---|---|---|---|---|---|---|---|
| Φ Avg | ΦN | ΦD | Pb | Φ S | Δt | | |
| 33.60992 | 21 | 31.51515 | 2.13 | 48.31461 | 120 | 1209 | 4.5 |
| 30.20202 | 30 | 27.27273 | 2.2 | 33.33333 | 100 | 1250 | 4.6 |
| 12.66088 | 15 | 12.12121 | 2.45 | 10.86142 | 70 | 1256 | 0.9 |
| 29.25253 | 32 | 22.42424 | 2.28 | 33.33333 | 100 | 1261 | 1.7 |
| 32.62785 | 32 | 30.30303 | 2.15 | 35.58052 | 103 | 1271 | 2 |
| 32.79265 | 28 | 30.30303 | 2.15 | 40.07491 | 109 | 1274 | 8 |
| 28.52525 | 28 | 24.24242 | 2.25 | 33.33333 | 100 | 1313 | 1.7 |
| 31.8545 | 30 | 28.48485 | 2.18 | 37.07865 | 105 | 1319 | 1.5 |
| 26.96527 | 23 | 26.06061 | 2.22 | 31.83521 | 98 | 1323 | 6.7 |
| 26.01419 | 23 | 25.45455 | 2.23 | 29.58801 | 95 | 1329 | 0.8 |
| 25.77619 | 22 | 24.24242 | 2.25 | 31.08614 | 97 | 1332 | 3 |
| 28.18182 | 30 | 21.21212 | 2.3 | 33.33333 | 100 | 1338 | 0.5 |
| 27.52525 | 25 | 24.24242 | 2.25 | 33.33333 | 100 | 1340 | 7 |
| 26.95358 | 24 | 27.27273 | 2.2 | 29.58801 | 95 | 1349 | 5 |
| 24.35161 | 26 | 21.21212 | 2.3 | 25.8427 | 90 | 1354 | 5.7 |
| 28.02463 | 25 | 24.24242 | 2.25 | 34.83146 | 102 | 1367 | 2 |
| 28.46465 | 26 | 26.06061 | 2.22 | 33.33333 | 100 | 1373 | 2.3 |
| 28.52525 | 28 | 24.24242 | 2.25 | 33.33333 | 100 | 1377 | 2.5 |
| 29.47475 | 26 | 29.09091 | 2.17 | 33.33333 | 100 | 1380 | 2.5 |
| 29.20202 | 27 | 27.27273 | 2.2 | 33.33333 | 100 | 1383 | 5.5 |
| 31.87754 | 29 | 30.30303 | 2.15 | 36.32959 | 104 | 1389 | 3 |
| 30.25979 | 27 | 29.69697 | 2.16 | 34.0824 | 101 | 1394 | 6 |
| 28.53535 | 25 | 27.27273 | 2.2 | 33.33333 | 100 | 1405 | 2 |
| 30.20202 | 30 | 27.27273 | 2.2 | 33.33333 | 100 | 1410 | 1.7 |
| 26.69254 | 24 | 24.24242 | 2.25 | 31.83521 | 98 | 1416 | 6 |
| 30.49938 | 30 | 26.66667 | 2.21 | 34.83146 | 102 | 1419 | 2 |
| 34.89774 | 32 | 36.36364 | 2.05 | 36.32959 | 104 | 1426 | 1.8 |
| 29.20202 | 27 | 27.27273 | 2.2 | 33.33333 | 100 | 1435 | 0.9 |
| 30.21212 | 27 | 30.30303 | 2.15 | 33.33333 | 100 | 1438 | 7 |
| 30.21212 | 27 | 30.30303 | 2.15 | 33.33333 | 100 | 1441 | 4 |
| 28.86869 | 26 | 27.27273 | 2.2 | 33.33333 | 100 | 1448 | 0.6 |
| 31.21212 | 30 | 30.30303 | 2.15 | 33.33333 | 100 | 1458 | 0.6 |
| 27.86869 | 23 | 27.27273 | 2.2 | 33.33333 | 100 | 1462 | 1.5 |
| 29.20202 | 27 | 27.27273 | 2.2 | 33.33333 | 100 | 1465 | 5 |
| 30.64964 | 22 | 32.12121 | 2.12 | 37.82772 | 106 | 1490 | 6 |

Table 4.4: Excel sheet calculation for kaikange well-3

| resistivity logs | | | | | | lithology logs | | |
|---|---|---|---|---|---|---|---|---|
| SW % | SW | RT | RLLS | Rlld | Rmsfl | VSH | I | Grlog |
| 29.78417 | 0.297842 | 6.2 | 30 | 35 | 0.6 | 0.085774 | 0.166667 | 65 |
| 11.05542 | 0.110554 | 45 | 45 | 110 | 0.7 | 0.139873 | 0.254902 | 74 |
| 10.79469 | 0.107947 | 47.2 | 120 | 135 | 30 | 0.103077 | 0.196078 | 68 |
| 25.742 | 0.25742 | 8.3 | 30 | 30 | 0.8 | 0.097231 | 0.186275 | 67 |
| 13.96056 | 0.139606 | 28.22 | 8 | 20 | 0.4 | 0.063774 | 0.127451 | 61 |
| 14.02031 | 0.140203 | 27.98 | 6 | 20 | 0.6 | 0.109003 | 0.205882 | 69 |
| 18.72873 | 0.187287 | 15.68 | 10 | 12 | 2 | 0.058458 | 0.117647 | 60 |
| 10.1735 | 0.101735 | 53.14 | 14 | 35 | 0.8 | 0.139873 | 0.254902 | 74 |
| 9.704539 | 0.097045 | 58.4 | 20 | 40 | 4 | 0.097231 | 0.186275 | 67 |
| 9.671474 | 0.096715 | 58.8 | 18 | 40 | 4 | 0.139873 | 0.254902 | 74 |
| 10.043 | 0.10043 | 54.53 | 16 | 40 | 1.4 | 0.091463 | 0.176471 | 66 |
| 9.842007 | 0.09842 | 56.78 | 14 | 40 | 0.8 | 0.097231 | 0.186275 | 67 |
| 9.960238 | 0.099602 | 55.44 | 12 | 40 | 0.6 | 0.139873 | 0.254902 | 74 |
| 10.38883 | 0.103888 | 50.96 | 10 | 35 | 0.8 | 0.091463 | 0.176471 | 66 |
| 9.31695 | 0.093169 | 63.36 | 9 | 50 | 0.6 | 0.097231 | 0.186275 | 67 |
| 12.00227 | 0.120023 | 38.18 | 8 | 30 | 0.4 | 0.058458 | 0.117647 | 60 |
| 12.56081 | 0.125608 | 34.86 | 10 | 30 | 0.4 | 0.069162 | 0.137255 | 62 |
| 10.25782 | 0.102578 | 52.27 | 12 | 40 | 0.6 | 0.103077 | 0.196078 | 68 |
| 11.74956 | 0.117496 | 39.84 | 10 | 30 | 0.4 | 0.109003 | 0.205882 | 69 |
| 10.87798 | 0.10878 | 46.48 | 8 | 40 | 0.4 | 0.139873 | 0.254902 | 74 |
| 10.38883 | 0.103888 | 50.96 | 14 | 38 | 0.8 | 0.11501 | 0.215686 | 70 |
| 10.75829 | 0.107583 | 47.52 | 10 | 35 | 0.6 | 0.097231 | 0.186275 | 67 |
| 14.0153 | 0.140153 | 28 | 4 | 20 | 0.4 | 0.103077 | 0.196078 | 68 |
| 13.65433 | 0.136543 | 29.5 | 7 | 21 | 0.5 | 0.11501 | 0.215686 | 70 |
| 10.13922 | 0.101392 | 53.5 | 19 | 40 | 0.6 | 0.085774 | 0.166667 | 65 |
| 14.98298 | 0.14983 | 24.5 | 7 | 20 | 0.4 | 0.11501 | 0.215686 | 70 |
| 14.32564 | 0.143256 | 26.8 | 5 | 20 | 0.9 | 0.074624 | 0.147059 | 63 |
| 13.58542 | 0.135854 | 29.8 | 3 | 18 | 0.3 | 0.109003 | 0.205882 | 69 |
| 15.66958 | 0.156696 | 22.4 | 3 | 15 | 0.4 | 0.074624 | 0.147059 | 63 |
| 14.14214 | 0.141421 | 27.5 | 3 | 17 | 0.6 | 0.069162 | 0.137255 | 62 |
| 19.02215 | 0.190221 | 15.2 | 2 | 9 | 0.6 | 0.053215 | 0.107843 | 59 |
| 11.27035 | 0.112703 | 43.3 | 15 | 30 | 0.5 | 0.085774 | 0.166667 | 65 |
| 15.43033 | 0.154303 | 23.1 | 4 | 15 | 0.4 | 0.063774 | 0.127451 | 61 |
| 17.43179 | 0.174318 | 18.1 | 4 | 10 | 0.5 | 0.058458 | 0.117647 | 60 |
| 14.32564 | 0.143256 | 26.8 | 5 | 20 | 0.4 | 0.074624 | 0.147059 | 63 |

Table 4.5: Excel sheet calculation for kaikange well-2

| porosity logs | | | | | | Depth | formation thickness |
|---|---|---|---|---|---|---|---|
| Φ Avg | ΦN | ΦD | Pb | Φ S | Δt | | |
| 28.70 | 27 | 27.27273 | 2.2 | 31.83521 | 98 | 1110 | 0.8 |
| 36.20 | 33 | 27.27273 | 2.2 | 48.31461 | 120 | 1172 | 0.9 |
| 38.72 | 36 | 33.33333 | 2.1 | 46.81648 | 118 | 1177 | 1.9 |
| 35.53 | 31 | 27.27273 | 2.2 | 48.31461 | 120 | 1200 | 4.5 |
| 40.22 | 39 | 33.33333 | 2.1 | 48.31461 | 120 | 1213 | 1.8 |
| 38.38 | 35 | 33.33333 | 2.1 | 46.81648 | 118 | 1215 | 2.2 |
| 35.44 | 27 | 27.27273 | 2.2 | 52.05993 | 125 | 1223 | 4.6 |
| 42.29 | 34 | 33.33333 | 2.1 | 59.55056 | 135 | 1234 | 1 |
| 42.96 | 36 | 33.33333 | 2.1 | 59.55056 | 135 | 1237 | 2.5 |
| 34.20 | 33 | 27.27273 | 2.2 | 42.3221 | 112 | 1252 | 2.4 |
| 40.22 | 39 | 33.33333 | 2.1 | 48.31461 | 120 | 1274 | 3.5 |
| 35.72 | 33 | 33.33333 | 2.1 | 40.82397 | 110 | 1278 | 1 |
| 35.71 | 36 | 30.30303 | 2.15 | 40.82397 | 110 | 1280 | 4 |
| 33.70 | 33 | 27.27273 | 2.2 | 40.82397 | 110 | 1285 | 3 |
| 32.46 | 30 | 30.30303 | 2.15 | 37.07865 | 105 | 1289 | 2.7 |
| 33.71 | 30 | 30.30303 | 2.15 | 40.82397 | 110 | 1292 | 5 |
| 32.04 | 28 | 30.30303 | 2.15 | 37.82772 | 106 | 1298 | 4.3 |
| 34.71 | 33 | 30.30303 | 2.15 | 40.82397 | 110 | 1305 | 7.3 |
| 31.01 | 30 | 29.69697 | 2.16 | 33.33333 | 100 | 1314 | 7 |
| 33.54 | 30 | 26.06061 | 2.22 | 44.56929 | 115 | 1323 | 10 |
| 35.21 | 36 | 30.30303 | 2.15 | 39.32584 | 108 | 1334 | 1 |
| 34.71 | 33 | 30.30303 | 2.15 | 40.82397 | 110 | 1336 | 12.5 |
| 33.71 | 30 | 30.30303 | 2.15 | 40.82397 | 110 | 1349 | 7 |
| 34.03 | 28 | 27.27273 | 2.2 | 46.81648 | 118 | 1356 | 11 |
| 31.45 | 30 | 27.27273 | 2.2 | 37.07865 | 105 | 1358 | 1.2 |
| 31.42 | 39 | 18.18182 | 2.35 | 37.07865 | 105 | 1371 | 2 |
| 31.19 | 30 | 24.24242 | 2.25 | 39.32584 | 108 | 1382 | 5 |
| 33.04 | 28 | 30.30303 | 2.15 | 40.82397 | 110 | 1385 | 5 |
| 35.78 | 29 | 31.51515 | 2.13 | 46.81648 | 118 | 1390 | 1.8 |
| 24.65 | 21 | 12.12121 | 2.45 | 40.82397 | 110 | 1395 | 8 |
| 26.71 | 27 | 27.27273 | 2.2 | 25.8427 | 90 | 1405 | 2 |
| 25.18 | 21 | 21.21212 | 2.3 | 33.33333 | 100 | 1410 | 2.5 |
| 29.68 | 36 | 21.21212 | 2.3 | 31.83521 | 98 | 1426 | 13 |
| 27.76 | 34 | 18.18182 | 2.35 | 31.08614 | 97 | 1429 | 13 |
| 28.58 | 41 | 15.15152 | 2.4 | 29.58801 | 95 | 1434 | 0.8 |
| 31.93 | 42 | 21.21212 | 2.3 | 32.58427 | 99 | 1443 | 1 |
| 31.85 | 41 | 21.21212 | 2.3 | 33.33333 | 100 | 1458 | 3 |
| 28.92 | 39 | 18.18182 | 2.35 | 29.58801 | 95 | 1466 | 1.8 |
| 26.16 | 30 | 15.15152 | 2.4 | 33.33333 | 100 | 1470 | 22.5 |

Table 4.6: Excel sheet calculation for kaikange well-2

| Resistivity logs | | | | | | lithology log | | |
|---|---|---|---|---|---|---|---|---|
| SW% | SW | RT | RLLS | Rlld | Rmsfl | VSH | I | GR log |
| 29.55 | 0.295468 | 6.3 | 4 | 6 | 2 | 0.146818 | 0.265487 | 67 |
| 27.99 | 0.279906 | 7.02 | 19 | 19 | 6 | 0.10758 | 0.20354 | 60 |
| 28.44 | 0.284398 | 6.8 | 15 | 22 | 7 | 0.189575 | 0.327434 | 74 |
| 25.77 | 0.257731 | 8.28 | 1 | 16 | 9 | 0.146818 | 0.265487 | 67 |
| 25.29 | 0.25289 | 8.6 | 15 | 21 | 7 | 0.043073 | 0.088496 | 47 |
| 22.46 | 0.22463 | 10.9 | 40 | 42 | 8 | 0.146818 | 0.265487 | 67 |
| 22.16 | 0.221601 | 11.2 | 30 | 35 | 10 | 0.164694 | 0.292035 | 70 |
| 24.86 | 0.248592 | 8.9 | 10 | 12 | 9 | 0.123984 | 0.230088 | 63 |
| 20.89 | 0.208928 | 12.6 | 40 | 70 | 2 | 0.10758 | 0.20354 | 60 |
| 8.40 | 0.083972 | 78 | 60 | 100 | 10 | 0.146818 | 0.265487 | 67 |
| 11.39 | 0.113883 | 42.408 | 16 | 30 | 1.2 | 0.189575 | 0.327434 | 74 |
| 11.97 | 0.11966 | 38.412 | 20 | 28 | 1.8 | 0.10758 | 0.20354 | 60 |
| 10.01 | 0.100109 | 54.88 | 30 | 40 | 2 | 0.10758 | 0.20354 | 60 |
| 35.71 | 0.357143 | 4.312 | 30 | 35 | 4 | 0.096974 | 0.185841 | 58 |
| 8.59 | 0.085933 | 74.48 | 35 | 55 | 2 | 0.152704 | 0.274336 | 68 |
| 8.95 | 0.08954 | 68.6 | 30 | 50 | 2 | 0.086625 | 0.168142 | 56 |
| 8.27 | 0.08273 | 80.36 | 30 | 60 | 2 | 0.096974 | 0.185841 | 58 |
| 8.95 | 0.08954 | 68.6 | 30 | 50 | 2 | 0.10758 | 0.20354 | 60 |
| 8.37 | 0.083667 | 78.57 | 35 | 60 | 3 | 0.118449 | 0.221239 | 62 |
| 9.84 | 0.098368 | 56.84 | 20 | 40 | 2 | 0.146818 | 0.265487 | 67 |
| 15.57 | 0.155664 | 22.698 | 12 | 16 | 6 | 0.10758 | 0.20354 | 60 |
| 10.25 | 0.10247 | 52.38 | 18 | 38 | 1.8 | 0.10758 | 0.20354 | 60 |
| 9.72 | 0.097212 | 58.2 | 18 | 40 | 3 | 0.189575 | 0.327434 | 74 |
| 13.75 | 0.137479 | 29.1 | 20 | 40 | 2 | 0.123984 | 0.230088 | 63 |
| 9.84 | 0.098368 | 56.84 | 10 | 20 | 4 | 0.129588 | 0.238938 | 64 |
| 14.16 | 0.141576 | 27.44 | 6 | 7 | 4 | 0.18324 | 0.318584 | 73 |
| 29.61 | 0.296127 | 6.272 | 6 | 8 | 3.5 | 0.158662 | 0.283186 | 69 |
| 23.76 | 0.237582 | 9.744 | 18 | 30 | 2 | 0.10758 | 0.20354 | 60 |
| 14.16 | 0.141576 | 27.44 | 5 | 8 | 4 | 0.164694 | 0.292035 | 70 |
| 20.31 | 0.203142 | 13.328 | 8 | 10 | 1 | 0.123984 | 0.230088 | 63 |
| 20.34 | 0.203355 | 13.3 | 8 | 16 | 1 | 0.091768 | 0.176991 | 57 |
| 14.14 | 0.141421 | 27.5 | 6 | 8 | 2 | 0.146818 | 0.265487 | 67 |
| 20.18 | 0.201843 | 13.5 | 5 | 6 | 8 | 0.038524 | 0.079646 | 46 |
| 22.26 | 0.222597 | 11.1 | 7 | 10 | 5 | 0.18324 | 0.318584 | 73 |
| 27.92 | 0.279191 | 7.056 | 8 | 9 | 7 | 0.176982 | 0.309735 | 72 |
| 22.09 | 0.220912 | 11.27 | 7 | 9 | 6 | 0.1708 | 0.300885 | 71 |
| 24.83 | 0.248341 | 8.918 | 8 | 9 | 6 | 0.146818 | 0.265487 | 67 |
| 24.31 | 0.243056 | 9.31 | 7 | 8 | 2 | 0.10758 | 0.20354 | 60 |
| 23.94 | 0.239357 | 9.6 | 10 | 21 | 1 | 0.038524 | 0.079646 | 46 |

## 4.2 Interpretation

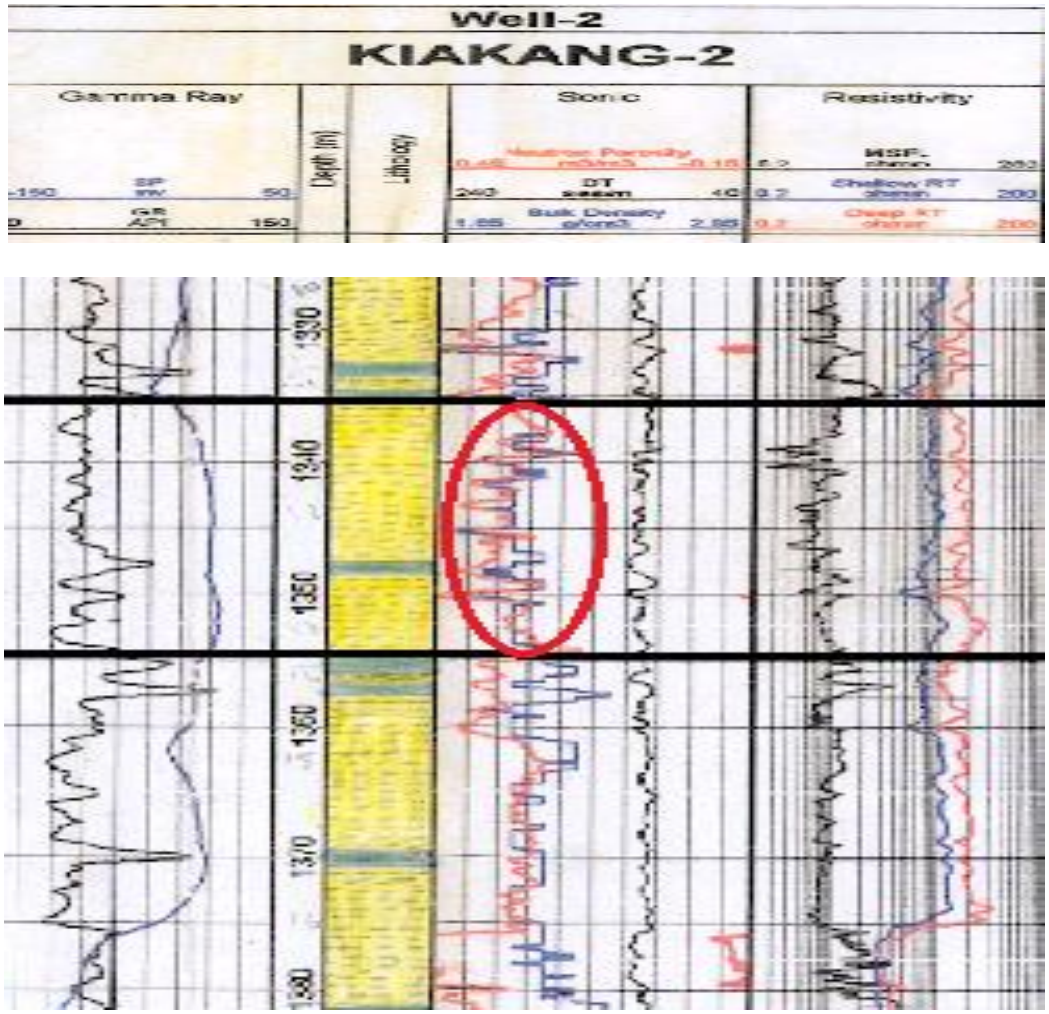


4.5 Figure: Shows zone of interest in kaikange well-2

The information obtained from sand zones illuminated in fig (4.5) summarized on the table below

Table 4.7: information of zone of interest in kaikange well-2

| The zone information | Value |
|---|---|
| Depth | 1336 |
| Thickness | 21m |
| Shale volume | 0.189575 |
| Average porosity | 35.7% |
| Water saturation | 10.25% |

From resistivity log the (**Rlld** & **Rlls**) curves represent high positive separation between them which indicate there may be oil in that zone.

In addition from the shape of cross-over of neutron and density curves gives other indicator for presence of oil.

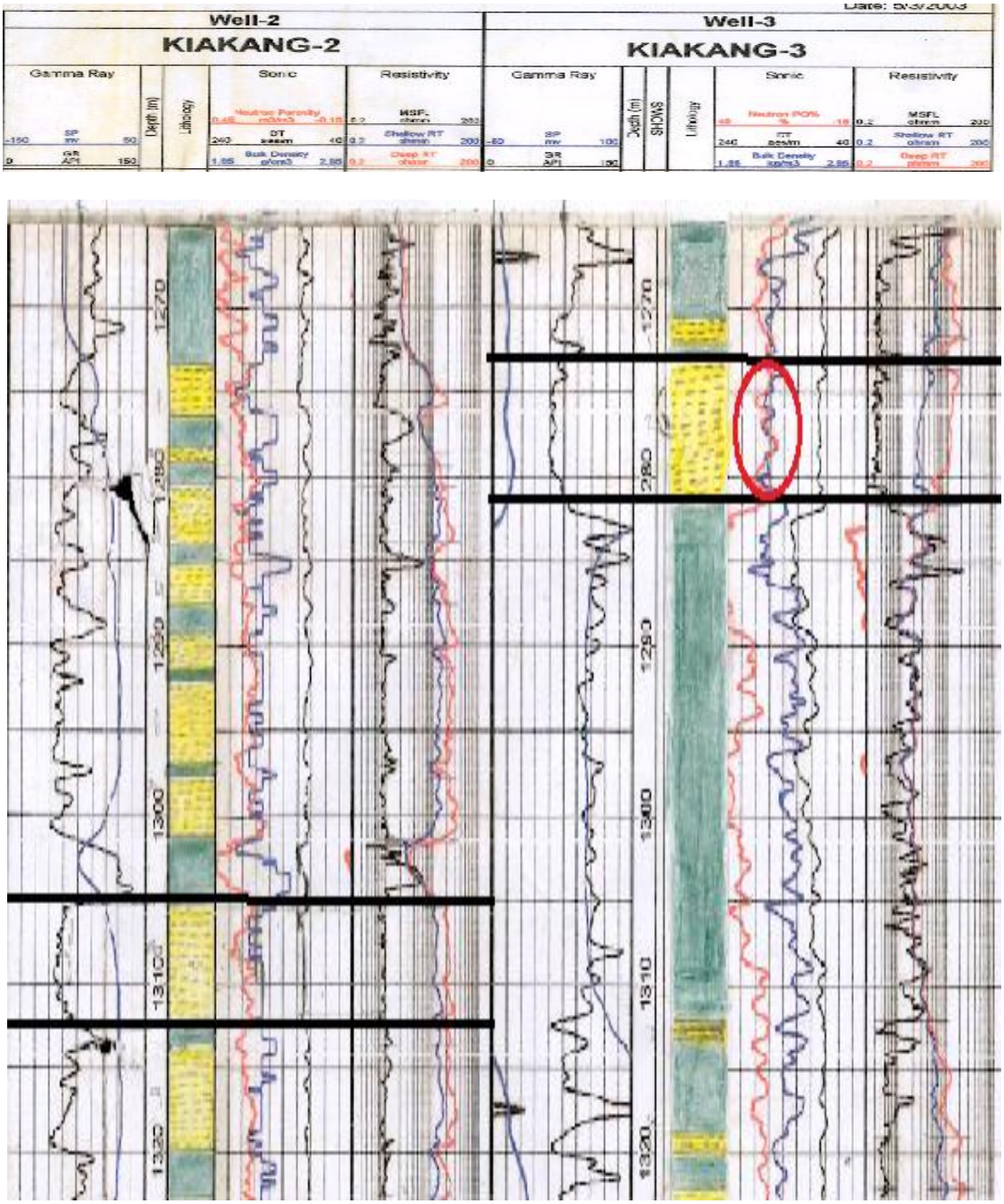


4.6 Figure: Shows two zones in kaikange well (2&3)

Figure (4.6) shows two zones in kaikange well-2 & kaikange well-3

In figure (4.6) the zone with red circle in kaikange well-3 has same interpretation as zone in kaikange well-2 in figure (4.6).

The information obtained from the other sand zone summarized on table below

Table 4.8: information of zone of interest in kaikange well-2

| The zone information | Value |
|---|---|
| Depth | 1305 |
| Thickness | 8m |
| Shale volume | 0.10758 |
| Average porosity | 35% |
| Water saturation | 15% |

From resistivity log the (**Rlld** & **Rlls**) curves represent low positive separation between them which indicate there may be fresh water in that zone.

In addition from the shape of neutron and density curves gives other indicator for presence of fresh water because there is no cross-over. Also the high reading of resistivity ensure the presence of fresh water in this zone.

# CHAPTER FIVE

# CONCLUSION AND RECOMMENDATION

# 5 Conclusion and Recommendation

## 5.1 Conclusion

Three wells from Muglad Basin namely, Kaikange well-1, kaikange well-2 and Kaikange well-3 were selected for well logging studies, to identify lithological character and determine some petrophysical properties of tendi formation.

In Kaikange well-1 there is 62 zones of sand stone determined by gamma ray log.The resistivity data are poor which there is not shallow focused resistivity reading. And this limited our work on only deep laterolog resistivity (Rlld) and micro spherically focus log.

In Kaikang well-2 the zone at depth 1335m had a good porosity ($\phi$ avg) and less water saturation (Sw) values. find out this zone can contain oil accumulation. Also same thing compatible on the zone at depth 1274m in kaikange well-3.

Generally, tendi formation relies on the data of three wells represents sand sequence with high porosity values range (25%-30%) and high water saturation content between (10%-20%).The oil also can take place, but with little amount in thinner zones.

## 5.2 Recommendation

From this study of wells we recommend to:

- We recommended to use of wireline logs together to get more accurate data.
- We recommended to use of mud logs with wireline logs to insure the results obtained from the study.
- We recommended to do more studies that focusing on the operations after drilling.

# 6 Reference

A.Y.Mohammed , W.A.Ashcroft and A. J. Whiteman (2001): Structural development and crustal stretching in the Muglad Basin, southern Sudan.

Ali Sayed Mohammed Ibrahim.(2003):Sedimentology and Reservoir Geology of the Middle-Upper Cretaceous Strata in Unity and Heglig Fields in SE Muglad Rift Basin, Sudan.

Avbovbo, J.A., E.O.Ayoola, and G.A.Osahon. (1986): Depositional and structure styles in Chad basin of northeastern Nigeria: AAPG Bulletin, v.70, p. 1787-1798

Browne, S .E .and J. D. Fairhead. (1983): Gravity study of the Central African rift system: a model of continental disruption; 1, theNgaoundere and Abu Gabra rift, P. Morgan, ed., Processes of continental rifting: Tectonophysics, v. 94, p. 187-203

Fairhead, J.D., 1986. Geophysical controls on sedi- mentation within the African rift systems. In: Frostlck, L.E., Renaut, R.W., Reid, I., Tlercehn, J.J. (Eds), Sedimentation in the African Rifts: Geologtcal Somety Special Publication 25, pp. 19-2

George Asquith with Charles Gibson. (1982): Basic well log analysis for geologists.

Girdler, J.D., Fairhead, R.C., Searle, and W.T.C. Sowerbutts. (1969): Evolution of rifting in Africa: Nature, v.224, p. 1178-1182

Mohamed, A.Y., Pearson, M. J., Ashcroft, W.A., Whiteman, A.J. (2002): Petroleum maturation modeling, AbuGabra- Sharaf area, MugladBasin, Sudan. Journal of African Earth Sciences 35, pp 331-344

Mann, D.C., 1989. Thick-skin and thin-skin detachment faults in continental Sudanese rift basins. Journal African Earth Sciences 8, 307-322.

Moniem, A., Yagoub, A., El Mustafa.A., Tayib.A, El Sharif. F., Mursi. H., Yousif. H., El Zein. L.A., Kehrer. P., Mamoon. A.R. (1984): Evaluation of petroleum wells. Program Released Within the Sudanese German Technical Cooperation (Unpublished Report) Geological and Mineral Resources Dept. (Sudan, 1984).

Mustafa, A.A., Tyson, R.V. (2002): Organic Facies of Early Cretaceous Synrift Lacustrine Source Rocks from the Muglad Basin, Sudan.Journal of Petroleum Geology Vol.25 (3), July 2002, pp 351-366..

Schull, T.J. (1988): Rift basins of interior Sudan: petroleum exploration
And discovery, AAPG Bull., 72, 1128-1142, Tulsa.

Robertson Research International Limted, (RRI) (1990): The Petroleum Potential of Southern, Central and Eastern Sudan. Vol.2 Geological and Stratigraphical Framework (Unpublished report).

Wright, J.D.(1981): Review of origin and evolution of the Benue trough in Nigeria: Earth Evolution Sciences, v. 2, p. 98-103.

# Appendix A

## LITHOLOGY INTERPERTATAION

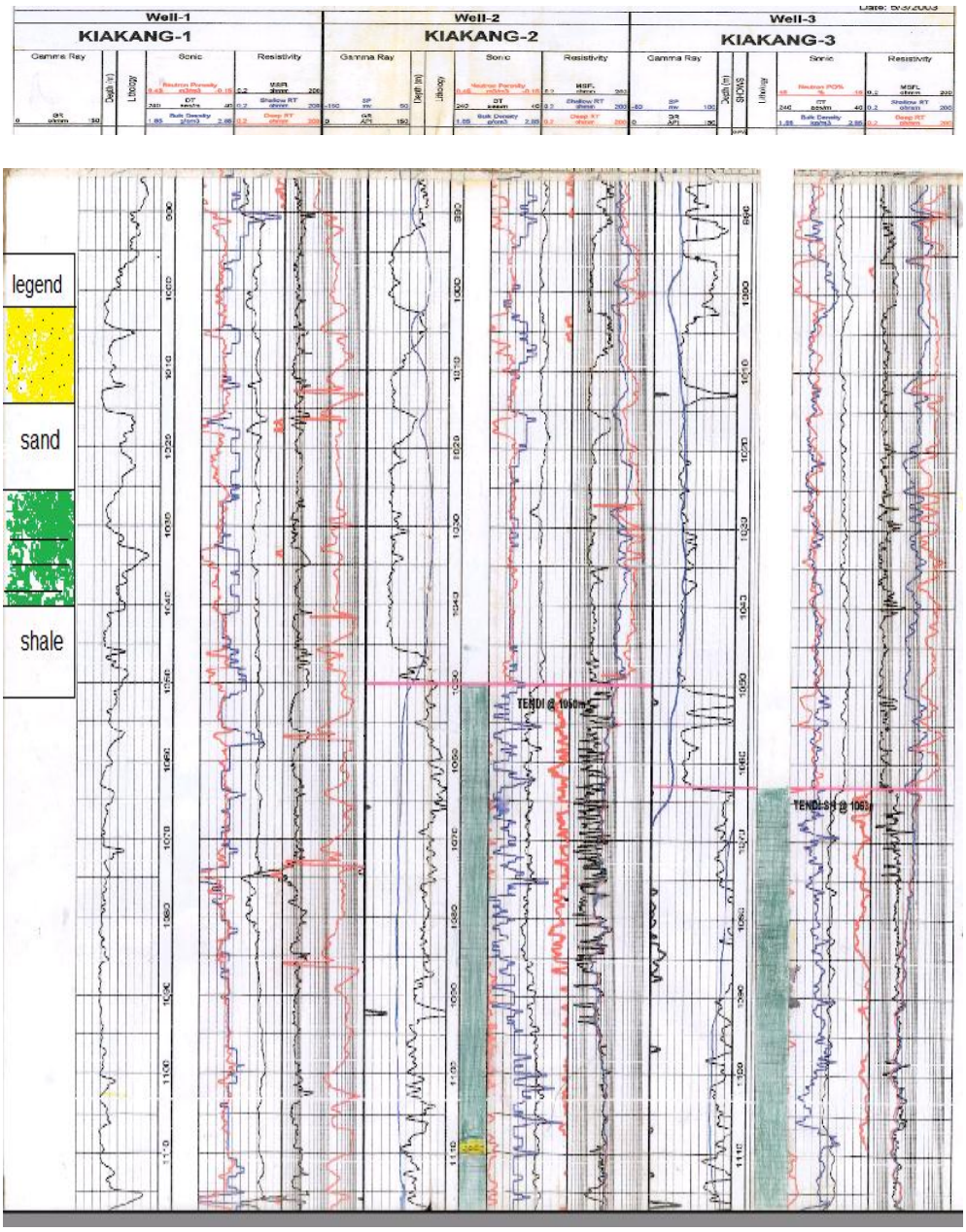
Well-1
KIAKANG-1
Well-2
KIAKANG-2
Well-3
KIAKANG-3
Gamma Ray
Sonic
Resistivity
legend
sand
shale
TENDI @ 1043m
TENDI-SS @ 1061m

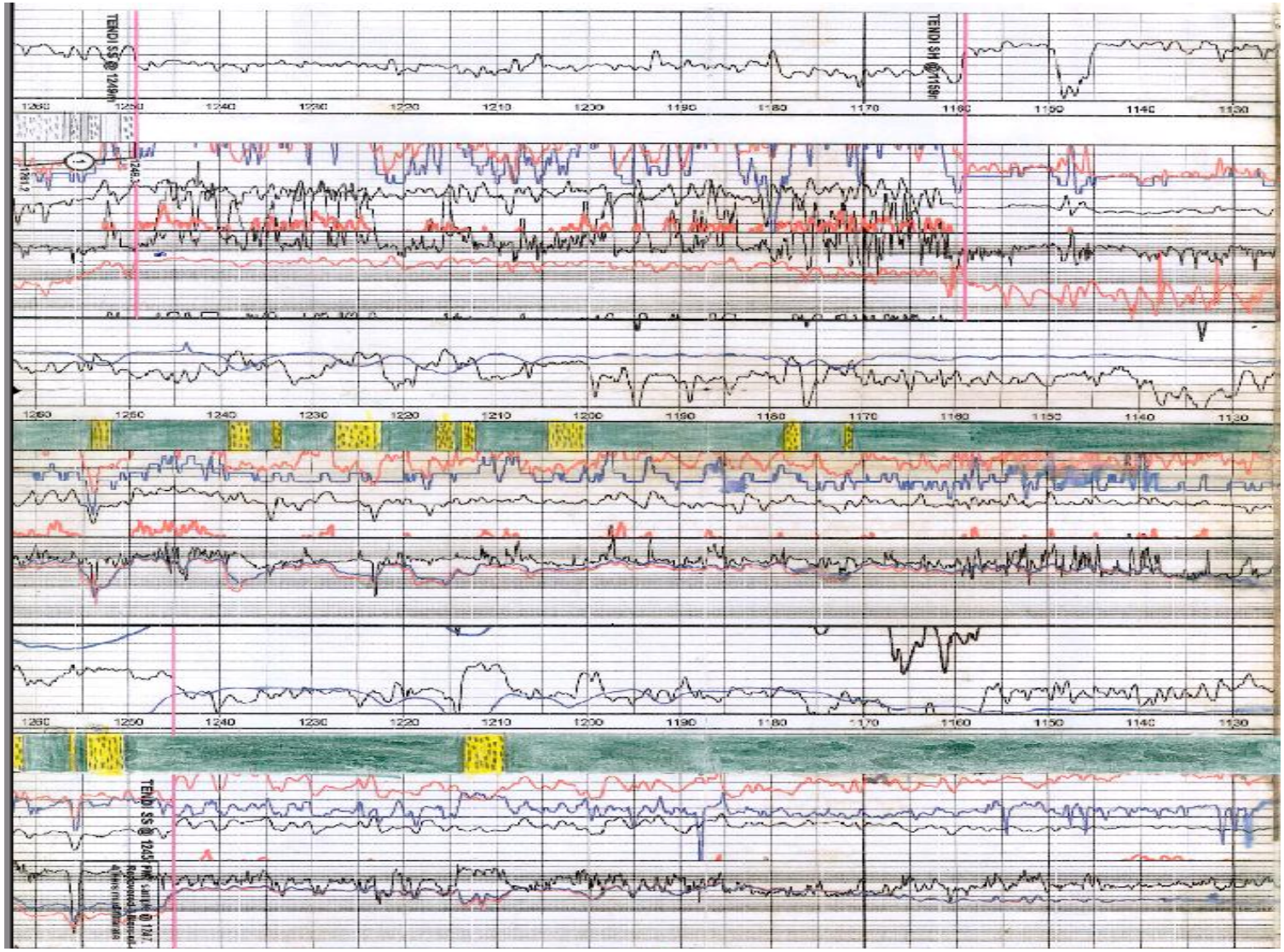
TEND1 SS @ 1249ft
TEND1 SH @ 1169ft
1260
1250
1240
1230
1220
1210
1200
1190
1180
1170
1160
1150
1140
1130
TEND SS @ 1245 PMC

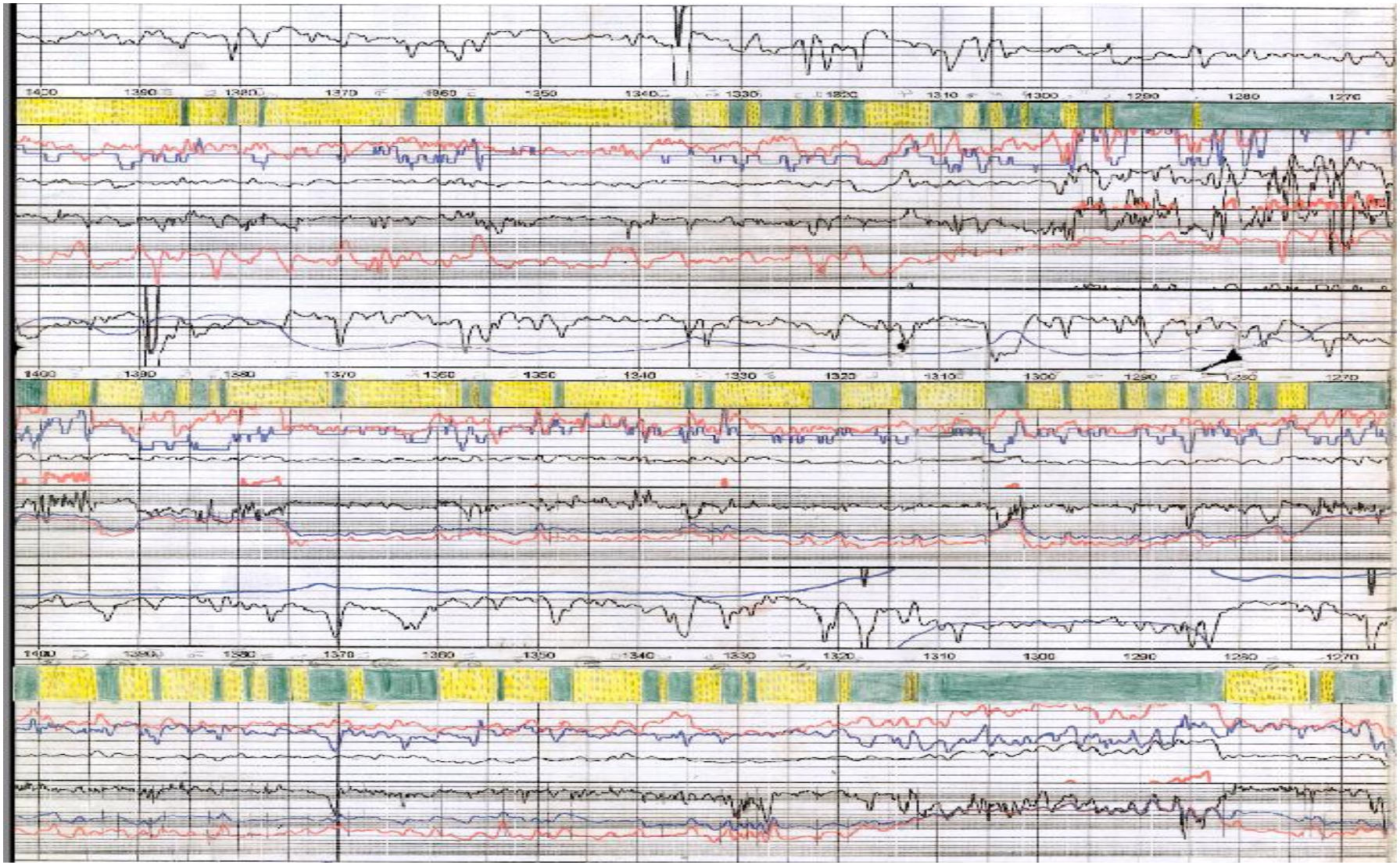

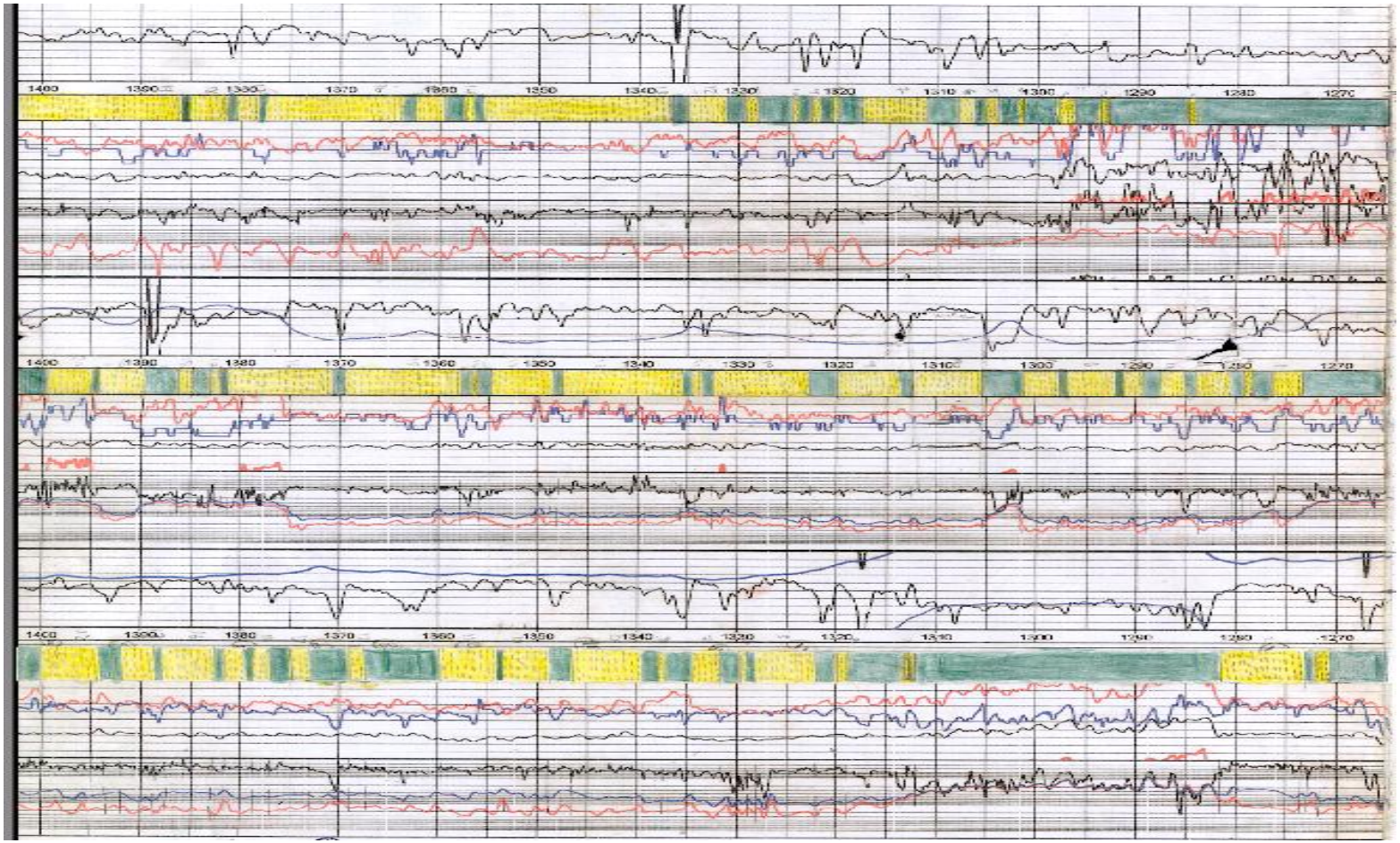

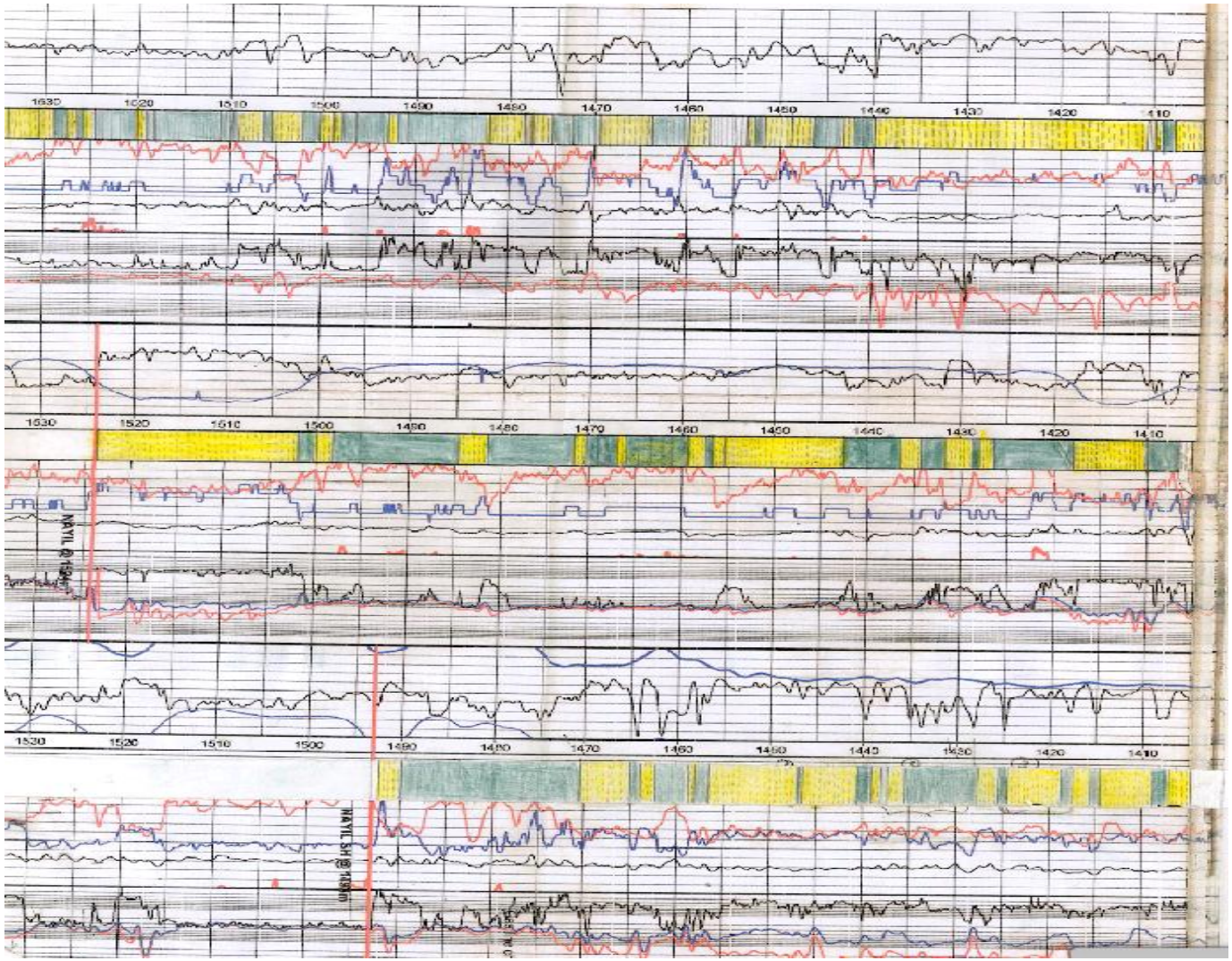
1530
1520
1510
1500
1490
1480
1470
1460
1450
1440
1430
1420
1410
NAYIL SH @ 1500
NAYIL SH @ 1500